lar weight heparin. Diabetes (2006) 55: 2510-2522.
22. Rauvala H and Pihlaskari R: Isolation and some characteristics of an adhesive factor of brain that enhances neurite outgrowth in central neurons. J Biol Chem (1987) 262: 16625-16635.
23. Merenmies J, Pihlaskari R, Laitinen J, Wartiovaara J and Rauvala H: 30-kDa heparin binding protein of brain (amphoterin) involved in neurite outgrowth. J Biol Chem (1991) 266: 16722-16729.
24. Rouhiainen A, Tumova S, Valmu L, Kalkkinen N and Rauvala H: Pivotal advance: analysis of proinflammatory activity of highly purified eukaryotic recombinant HMGB1 (amphoterin). J Leukoc Biol (2007) 81: 49-58.
25. Moroz OV, Antson AA, Dodson GG, Wilson KS, Skibshoj I, Lukanidin EM, Bronstein IB: Crystallization and preliminary X-ray diffraction analysis of human calcium-binding protein S100A12. Acta Crystallogr D Biol Crystallogr (2000) 56: 189-191.
26. Hofmann MA, Drury S, Fu C, Qu W, Taguchi A, Lu Y, Avila C, Kambham N, Bierhaus A, Nawroth P, Neurath MF, Slattery T, Beach D, McClary J, Nagashima M, Morser J, Stern D, Schmidt AM: RAGE mediates a novel proinflammatory axis: a central cell surface receptor for S100/calgranulin polypeptides. Cell (1999) 97: 889-901.
27. Hoppensteadt D, Walenga JM, Fareed J and Bick RL: Heparin, low-molecular-weight heparins, and heparin pentasaccharide: basic and clinical differentiation. Hematol Oncol Clin North Am (2003) 17: 313-341.
28. Spyropoulos AC: Pharmacologic therapy for the management of thrombosis: unfractionated heparin or low-molecular-weight heparin? Clin Cornerstone (2005) 7: 39-48.
29. Hoffart V, Lamprecht A, Maincent P, Lecompte T, Vigneron C and Ubrich N: Oral bioavailability of a low molecular weight heparin using a polymeric delivery system. J Control Release (2006) 113: 38-42.
30. Scheuch G, Brand P, Meyer T, Herpich C, Müllinger B, Brom J, Weidinger G, Kohlhäufl M, Häussinger K, Spannagl M, Schramm W and Siekmeier R: Anticoagulative effects of the inhaled low molecular weight heparin certoparin in healthy subjects. J Physiol Pharmacol (2007) 58 Suppl 5: 603-614.
31. Tyrrell DJ, Horne AP, Holme KR, Preuss JM and Page CP: Heparin in inflammation: potential therapeutic applications beyond anticoagulation. Adv Pharmacol (1999) 46: 151-208.
32. Wang L, Brown JR, Varki A and Esko JD: Heparin's anti-inflammatory effects require glucosamine 6-O-sulfation and are mediated by blockade of L- and P-selectins. J Clin Invest (2002) 110: 127-136.
33. Fareed J, Hoppensteadt DA and Bick RL: An update on heparins at the beginning of the new millennium. Semin Thromb Hemost (2000) 26: 5-21.
34. Esmon CT: Coagulation inhibitors in inflammation. Biochem Soc Trans (2005) 33: 401-405.
35. Schouten M, Wiersinga WJ, Levi M and van der Poll T: Inflammation, endothelium, and coagulation in sepsis. J Leukoc Biol (2008) 83: 536-545.
36. Jaimes F and de la Rosa G: Anticoagulation and sepsis: the opportunity for a new use of heparin? Biomedica (2006) 26: 150-160.
37. Okajima K: Regulation of inflammatory responses by natural anticoagulants. Immunol Rev (2001) 184: 258-274.
38. Clynes R, Moser B, Yan SF, Ramasamy R, Herold K and Schmidt AM: Receptor for AGE (RAGE): weaving tangled webs within the inflammatory response. Curr Mol Med (2007) 7: 743-751.
39. Yan SF, Ramasamy R, Naka Y and Schmidt AM: Glycation, inflammation, and RAGE: a scaffold for the macrovascular complications of diabetes and beyond. Circ Res (2003) 93: 1159-1169.
40. Orlova VV, Choi EY, Xie C, Chavakis E, Bierhaus A, Ihanus E, Ballantyne CM, Gahmberg CG, Bianchi ME, Nawroth PP and Chavakis T: A novel pathway of HMGB1-mediated inflammatory cell recruitment that requires Mac-1-integrin. EMBO J (2007) 26: 1129-1139.

European Journal of Pharmacology 623 (2009) 89–95

Contents lists available at ScienceDirect

European Journal of Pharmacology

journal homepage: www.elsevier.com/locate/ejphar

Cardiovascular Pharmacology

Histidine-rich glycoprotein inhibited high mobility group box 1 in complex with heparin-induced angiogenesis in matrigel plug assay

Hidenori Wake [a], Shuji Mori [b], Keyue Liu [a], Hideo K. Takahashi [a], Masahiro Nishibori [a,*]

[a] Department of Pharmacology, Okayama University Graduate School of Medicine, Dentistry and Pharmaceutical Sciences, Okayama 700-8558, Japan
[b] Shujitsu University, School of Pharmacy, Okayama 703-8516, Japan

ARTICLE INFO

Article history:
Received 7 May 2009
Received in revised form 28 August 2009
Accepted 8 September 2009
Available online 26 September 2009

Keywords:
Angiogenesis
HMGB1
HRG
Heparin

ABSTRACT

Histidine-rich glycoprotein (HRG) is a heparin-binding glycoprotein present in plasma at 100 μg/ml. A recent study revealed that HRG suppressed heparin-dependent basic fibroblast growth factor (bFGF)-induced angiogenesis. Additionally, we reported that high mobility group box 1 (HMGB1) in complex with heparin induces angiogenesis; therefore, we examined the effect of HRG on heparin-dependent HMGB1-induced angiogenesis in the present study. HRG completely inhibited angiogenesis induced by HMGB1 in complex with heparin. HRG inhibited the diffusion of a complex of HMGB1 with heparin from matrigel into surrounding tissue. HRG also competed with HMGB1 for heparin binding *in vitro*. Moreover, HRG inhibited heparin-dependent vascular endothelial growth factor-A_{165} (VEGF-A_{165})-induced angiogenesis. These results strongly suggested that HRG might be an inhibitor of angiogenesis induced by growth factors with heparin binding activity and that HRG may be a potential drug for angiogenic diseases, including tumor growth.

© 2009 Elsevier B.V. All rights reserved.

1. Introduction

Histidine-rich glycoprotein (HRG) is mainly produced in the liver and is consistently present in plasma at considerable levels (100 μg/ml, 1.25 μM) (Rylatt et al., 1981; Drasin and Sahud, 1996). HRG is an 80 kDa glycoprotein and has four domains; cystatin-like domain 1, cystatin-like domain 2, histidine–proline-rich domain and C-terminal domain. The histidine–proline-rich domain has a characteristic 12 times amino acid sequence repeat of GHHPH, whose physiological significance remains unclear (Koide et al., 1986). *In vitro* studies revealed that HRG has affinity for a variety of substances, including heparin, heparan sulfate proteoglycan (Lijnen et al., 1983; Burch et al., 1987; Peterson et al., 1987), plasminogen (Lijnen et al., 1980), thrombospnodin (Leung et al., 1984; Silverstein et al., 1985), fibrinogen, fibrin (Leung, 1986), divalent metal ions (Morgan, 1981; Guthans and Morgan, 1982), heme (Morgan, 1985) and complement C1q (Gorgani et al., 1997), suggesting that HRG may play roles relating to the control of coagulation and the fibrinolysis and immune systems; however, its functional significance has not yet been clarified. Moreover, HRG was reported to suppress vascular endothelial growth factor (VEGF) and basic fibroblast growth factor (bFGF)-induced angiogenesis, suggesting that HRG plays an important role in maintaining blood vessel homeostasis in collaboration with angiogenic growth factors (Juarez et al., 2002; Doñate et al., 2004; Guan et al., 2004; Olsson et al., 2004).

High mobility group box 1 (HMGB1) is a non-histone nuclear protein, which maintains the architecture of chromatin DNA and regulates transcription (Bustin, 1999; Yuan et al., 2004). HMGB1 is released from necrotic cells and activated macrophages. Once released into extracellular space, it acts as pro-inflammatory cytokine (Wang et al., 1999, 2001; Scaffidi et al., 2002). HMGB1 is highly expressed in inflammatory conditions, such as sepsis (Karlsson et al., 2008), rheumatic arthritis (Taniguchi et al., 2003) and atherosclerosis (Porto et al., 2006). Recent studies revealed that HMGB1 induced the sprouting and chemotaxis of vascular endothelial cells and promoted angiogenesis in the chick embryo chorioallantoic membrane (Schlueter et al., 2005; Mitola et al., 2006). Moreover, in the previous study, we demonstrated that HMGB1 complexed with heparin induced angiogenesis in a matrigel plug assay (Wake et al., 2009).

In the present study, we analyzed the effects of HRG on HMGB1-induced angiogenesis in terms of the competition for heparin binding, and the expression of tumor necrosis factor-α (TNF-α) and VEGF-A_{120}.

2. Materials and methods

2.1. Reagents

Matrigel was prepared from the Engelbreth–Holm–Swarm sarcoma inoculated in C57BL/6J mice, as previously described (Kleinman

* Corresponding author. Tel./fax: +81 86 235 7140.
E-mail address: mbori@md.okayama-u.ac.jp (M. Nishibori).

0014-2999/$ – see front matter © 2009 Elsevier B.V. All rights reserved.
doi:10.1016/j.ejphar.2009.09.010

et al., 1986). Matrigel was not supplemented with any growth factors and mainly contained laminin, collagen IV, heparan sulfate proteoglycan and entactin. Since matrigel is liquid at 4 °C and becomes a gel at 22–35 °C, we injected the ice-cold matrigel solution into the back of mice, enabling gel formation subcutaneously. Rabbit polyclonal antibody against human HRG was raised by immunization of a rabbit with human HRG purified from plasma. Rat monoclonal anti-bovine HMGB1 antibody (#10–22) was produced as previously described (Liu et al., 2007).

2.2. Animals

All animal experiments were performed in accordance with the guidelines of Okayama University on animal experiments, approved by the University's committee on animal experimentation, and conformed to the Guide for the Care and Use of Laboratory Animals published by the US National Institutes of Health (NIH Publication No. 85-23, revised 1996). Male C57BL/6J mice (24–26 g, 7–8 weeks) were obtained from the animal resources of Okayama University. Mice were housed at 22 °C and relative humidity with a regular 12-h light–dark schedule. Food and water were available *ad libitum*.

2.3. Expression and purification of recombinant human HMGB1

Recombinant human HMGB1 was produced as described previously (Wake et al., 2009). In brief, the complementary DNA (cDNA) encoding full-length HMGB1 was amplified by polymerase chain reaction (PCR) from a human microvascular endothelial cell cDNA using primers. The PCR product was subcloned into pGEX-6p-1 vector (GE Healthcare, Little Chalfont, England). The recombinant plasmids were transformed into *E. coli* strain BL21 (DE3) (Merck, San Diego, LA) and incubated overnight at 37 °C in Overnight Express Instant TB medium (Merck, San Diego, LA) to express recombinant glutathione S-transferase (GST)-HMGB1. *E. coli* extract containing GST-HMGB1 fusion proteins was incubated with glutathione-Sepharose 4B for 1 h at room temperature. After washing, the gel bed was incubated with PreScission protease for 3 h at 4 °C. After brief centrifugation, the supernatant containing GST-tag-deleted HMGB1 was collected and purified by gel filtration chromatography using TSK-gel 3000SW$_{XL}$ (Tosoh, Tokyo, Japan). Purified recombinant human HMGB1 protein was identified by Western blotting (Towbin et al., 1979) with anti-HMGB1 monoclonal antibody (#10–22). Lipopolysaccharide (LPS) content in purified recombinant human HMGB1 was less than 2.0 pg/μg protein.

2.4. Purification of HRG from human plasma

HRG was purified from human plasma, as previously described (Mori et al., 2003). In brief, human plasma was incubated with nickel-nitrilotriacetic acid (Ni-NTA) agarose (Qiagen, Hilden, Germany) for 2 h at 4 °C with gentle shaking. The gel was packed into a column and washed successively with 10 mM Tris-buffered saline (TBS) (pH 8.0) containing 10 mM imidazole, and then 10 mM Tris-buffer (TB) (pH 8.0) containing 1 M NaCl. Human HRG was eluted by 0.5 M imidazole in 10 mM TBS (pH 8.0). The protein extract was further purified by fast protein liquid chromatography (FPLC) using a Mono Q column (GE Healthcare, Little Chalfont, UK) with NaCl gradient. Purified human HRG was identified by sodium dodecyl sulfate-polyacrylamide gel electrophoresis (SDS-PAGE) and Western blotting with human HRG specific antibody.

2.5. Evaluation of angiogenesis using matrigel plug assay

Matrigel is a basement membrane component mixture and is liquid at 4 °C. Male C57BL/6J mice were anesthetized with 50% N_2O + 50% O_2, and 500 μl liquid matrigel mixture at 4 °C was injected subcutaneously into the back using a 25G needle. The matrigel mixture contained phosphate buffered saline (PBS), HMGB1 (2.5 μg/ml, 100 nM), heparin (64 units/ml) (Sigma, St. Louis, MO), HRG (100 μg/ml, 1.25 μM), heparin + HMGB1, heparin + HMGB1 + HRG, human VEGF-A_{121} (185 ng/ml, 6.5 nM) or (1.85 μg/ml, 65 nM) (Peprotech, Rocky Hill, CT), human VEGF-A_{165} (250 ng/ml, 6.5 nM) (Peprotech,), human VEGF-A_{121} + heparin, human VEGF-A_{165} + heparin, human VEGF-A_{121} + HRG, human VEGF-A_{165} + HRG, human VEGF-A_{121} + heparin + HRG or human VEGF-A_{165} + heparin + HRG. The liquid matrigel mixture solidified 5–10 min after inoculation. After 10 days, mice were sacrificed by cervical dislocation and the matrigel plugs were removed and photographed. To evaluate angiogenesis, the hemoglobin content of the removed matrigel plug was measured using a Hemoglobin B test kit (Wako, Osaka, Japan). The matrigel plug was homogenized in 10 mM PBS (pH 7.4) and centrifuged at 8000×g for 10 min. The supernatant was mixed with hemoglobin coloring reagent and incubated for 3 min at room temperature. Absorbance was measured at 540 nm. The total hemoglobin concentration was estimated by the standard curve using hemoglobin standard reagent. Additionally, the plugs were fixed with 10% formalin in 0.1 M phosphate buffer and stained with hematoxylin–eosin on 5 μm paraffin sections. Microvessels in the plug were assessed by CD31 immunostaining of 5 μm paraffin sections. After deparaffinization and blocking, the sections were incubated with rabbit polyclonal anti-mouse CD31 antibody (Abcam, Cambridge, UK) at 4 μg/ml followed by anti-rabbit IgG goat IgG-horseradish peroxidase (HRP) (Abcam). Immunoreactivity was visualized with 0.05% 3,3′-diaminobenzidine (Sigma) and 0.03% H_2O_2. Nuclei were counterstained with Mayer's hematoxylin. A negative control for immunohistochemical staining was obtained with the same concentration of normal rabbit IgG. The number of CD31-positive vessels was counted in 5 fields of the matrigel plug section under a microscope at 400× magnification. Microvessel density (MVD) was expressed as the number of microvessels per square millimeter.

2.6. Competition between HMGB1 and HRG using heparin-binding plate

Heparin (5 units/ml) in 10 mM PBS (pH 7.4) was added to a heparin binding plate (BD, Franklin Lakes, NJ). After three washings with acetate buffer (100 mM NaCl, 50 mM NaAc, 0.2% Tween-20 pH 7.2), 0.2% gelatin solution (Sigma) was added to wells to block nonspecific binding. Each concentration of HMGB1 (0, 5 and 10 μg/ml) and HRG (0, 10, 50 and 100 μg/ml) was added to the well and incubated at 37 °C for 2 h. After washing, 0.5 μg/ml anti-HMGB1 monoclonal antibody (R&D Systems, Minneapolis, MN) was added to wells followed by the addition of anti-mouse IgG goat polyclonal IgG-HRP (MBL, Nagoya, Japan) to determine bound HMGB1. The reaction was developed by ABTS and H_2O_2 and determined at 405 nm using a microplate reader model 680 (Bio-rad, Hercules, CA).

2.7. Western blot analysis of HMGB1 levels in matrigel plug

Matrigel mixture that contained PBS, HMGB1 (2.5 μg/ml, 100 nM), heparin (64 units/ml) + HMGB1 or heparin + HMGB1 + HRG (100 μg/ml, 1.25 μM) was injected subcutaneously into the back. After 1, 3 or 10 days, mice were sacrificed and the matrigel plugs were removed. Equal amounts of matrigel homogenate sample corresponding to 2.5 mg wet weight were electrophoresed on polyacrylamide gel (12.5%) and transferred onto a polyvinylidine difloride (PVDF) membrane (Bio-rad). After the membrane was stained with Ponceau S, it was blocked with 10% skim milk for 1 h and incubated overnight at 4 °C with mouse monoclonal anti-human HMGB1 antibody (R&D Systems) followed by anti-mouse IgG goat polyclonal IgG-HRP (MBL, Nagoya, Japan) for 1 h at room temperature. The signals were finally visualized using the enhanced chemiluminescence system (Pierce Biotechnology, Rockford, IL).

2.8. Reverse transcription polymerase chain reaction (RT-PCR)

Mouse skin samples in contact with matrigels were dissected from the portion just above the gels as 5 mm square. Total RNA was purified from the skin sample using an RNeasy fibrous tissue mini kit (Qiagen, Hilden, Germany) and cDNA was synthesized using Takara RNA PCR kit Ver. 3.0 (Takara Bio, Nagahama, Japan) according to the manufacturer's instructions. PCR was performed in a PCR Thermal Cycler (Takara Bio) using Ex Taq DNA polymerase HS (Takara Bio), and sequence-specific primers according to the conditions described previously (Wake et al., 2009). The PCR product was electrophoresed on 2% agarose gel.

2.9. Real-time quantitative PCR

Real-time PCR was performed with a Light Cycler (Roche, Basel, Swiss) using SYBR premix Ex Taq (Takara Bio, Shiga, Japan) and cDNA from mouse skin and sequence-specific primers (Wake et al., 2009), according to the manufacturer's instructions. The expression of glyceraldehyde-3-phospate dehydrogenase (GAPDH) was used to normalize cDNA levels. The PCR products were analyzed by a melting curve to ascertain the specificity of amplification.

2.10. Statistical analysis

For each experiment, data are presented as the means ± S.E.M. The results were analyzed by one-way analysis of variance (one-way ANOVA) followed by Student's *t*-test. *P* values < 0.05 were considered significant.

3. Results

3.1. Effect of HRG on HMGB1-induced angiogenesis in the presence of heparin using matrigel plug assay

We investigated the anti-angiogenic effects of HRG on HMGB1-induced angiogenesis in the presence of heparin using a matrigel plug assay. Matrigel mixture was implanted subcutaneously into the back. After 10 days, the matrigel plugs were removed. The matrigel plug treated with PBS, HMGB1 or HRG alone was pale in color, whereas the matrigel plug treated with heparin alone was slightly red; however, the matrigel plug treated with a combination of HMGB1 and heparin was very red and the hemoglobin content of this plug was significantly increased, indicating that HMGB1-induced angiogenesis was heparin-dependent. The addition of HRG to the combination of HMGB1 and heparin almost completely inhibited the increase in hemoglobin content induced by the combination (Fig. 1A, B). A thin section of matrigel was stained with hematoxylin–eosin and anti-CD31 antibody. In the group treated with a combination of HMGB1 and heparin, CD31-positive luminal structures and many infiltrating cells, including leukocytes, were observed in the plug (Fig. 2A panels e, k); however, a few CD31-positive structures and infiltrating cells in the gel were observed in sections from other groups (Fig. 2A panels a–d, f, g–j, l). The number of CD31-positive microvessels was counted in five random fields. In the plug treated with the combination of HMGB1 and heparin, CD31-positive microvessels were significantly increased compared to those by HMGB1, heparin and HRG alone. HRG completely inhibited the increase in CD31-positive microvessels induced by the combination. There was a significant correlation between the hemoglobin contents and the number of CD31-positive microvessels. Collectively, it was suggested that HRG inhibited the migration activity of vascular endothelial cells as well as leukocytes induced by the combination of HMGB1 and heparin (Fig. 2B).

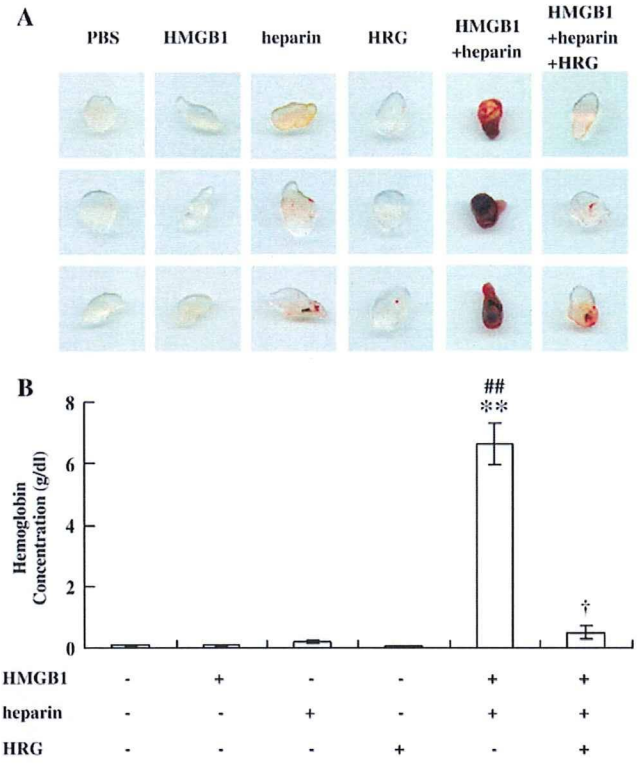

Fig. 1. Effect of HRG on the angiogenesis induced by HMGB1 and heparin using matrigel assay. (A) Matrigel mixture contained HMGB1, HRG and heparin alone or in combination. Ten days after inoculation, the matrigel plugs were recovered. Each group consisted of 6 mice. (B) Hemoglobin content in matrigel plugs was determined. Data are the means ± S.E.M. of 6 matrigels. $^{**}P<0.01$ *vs.* PBS control; $^{\#\#}P<0.01$ *vs.* heparin alone; $^{\dagger}P<0.05$ *vs.* combination of HMGB1 and heparin.

3.2. Competition between HRG and HMGB1 for heparin binding

To evaluate the inhibitory effect of HRG on HMGB1–heparin binding, we performed a competitive binding assay using a heparin-binding plate. The molar ratios of HRG/HMGB1, ranging from 0.3 to 6.3, were examined. The addition of increasing concentrations of HRG inhibited HMGB1–heparin binding in a concentration-dependent manner. One hundred micrograms/milliliter HRG (normal human plasma concentration) inhibited HMGB1 (5 μg/ml: twice the concentration of HMGB1 in matrigel plug assay)–heparin binding by 75% (Fig. 3).

3.3. Determination of HMGB1 levels in matrigel

To identify the degradation of HMGB1 in matrigel and its diffusion from gel, we detected HMGB1 in plugs recovered 1, 3 and 10 days after inoculation using Western blot analysis. Each matrigel mixture contained PBS, HMGB1, heparin + HMGB1 and heparin + HMGB1 + HRG, respectively. The same amount of matrigel homogenate was loaded onto each lane (Fig. 4A). In each matrigel plug recovered 1 day after inoculation, a constant level of HMGB1 was detected. After 3 days, HMGB1 was completely ablated in matrigel with HMGB1 and heparin. Such a disappearance was completely suppressed by the addition of HRG. HMGB1 levels did not significantly change in matrigel during a 10-day period except for HMGB1 and heparin groups (Fig. 4B). Moreover, no degradative bands were detected in each group throughout the period. These data suggested that HMGB1 in complex with heparin diffused into tissue surrounding matrigel and HRG completely suppressed its diffusion.

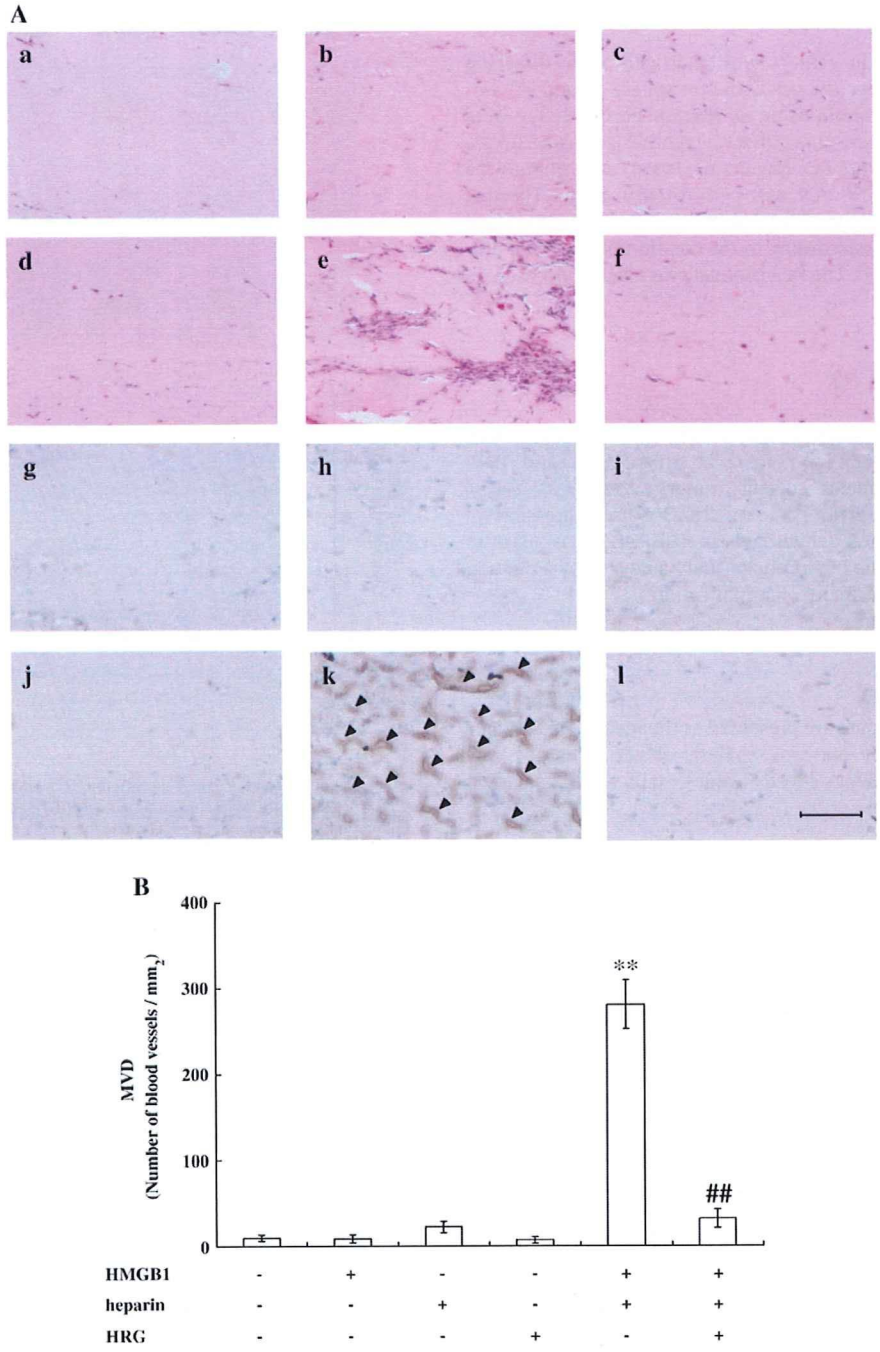

Fig. 2. Histological study of matrigel plug sections. (A) Matrigel plug sections were stained by hematoxylin–eosin (a–f) or by anti-CD31 antibody (g–l). Matrigels contained PBS (a,g), HMGB1 alone (b,h), heparin alone (c,i), HRG alone (d,j), a combination of HMGB1 and heparin (e,k), a combination of HMGB1, heparin and HRG (f,l). *Arrowheads* indicate CD31-positive blood vessels. Scale bar represents 100 μm. (B) Under a microscope, CD31-positive vessels were counted in 5 fields of a matrigel plug section at 400× magnification. Microvessel density (MVD) was expressed as the number of microvessels per square millimeter. Data are the means ± S.E.M. of 5 fields. $^{**}P<0.01$ *vs.* PBS control group. $^{\#\#}P<0.01$ *vs.* combination of HMGB1 and heparin.

3.4. HRG inhibited the expression of TNF-α and VEGF-A_{120} induced by the combination of HMGB1 and heparin

Ten days after inoculation of matrigel, total RNA was extracted from mouse skin surrounding matrigel. The expression of messenger RNA (mRNA) coding for cytokines, matrix metalloproteinases (MMPs) or growth factors was determined by RT-PCR. Treatment with a combination of HMGB1 and heparin significantly up-regulated the expressions of TNF-α and VEGF-A_{120} in mouse skin surrounding matrigel as compared with any groups receiving treatment with PBS, heparin, HMGB1 and HRG alone. The addition of HRG to the combination of HMGB1 and heparin abolished the enhanced expression of TNF-α and VEGF-A_{120} completely (Fig. 5A). In contrast, there were no significant differences in inducible nitric oxide synthase (iNOS), endothelial NOS (eNOS), MMP-2, MMP-9, VEGF receptor-1 (VEGFR-1), VEGFR-2, VEGF-A_{164}, VEGF-A_{188} and bFGF mRNA levels among groups (data not shown). The expression of TNF-α and VEGF-A_{120} mRNA was quantified using real-time PCR. Treatment of HMGB1 alone significantly increased the expression of

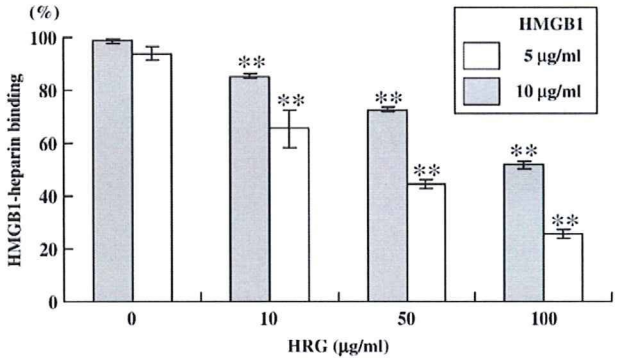

Fig. 3. HMGB1 binding to heparin. HMGB1 alone or in combination with indicated concentrations of HRG (10, 50 or 100 μg/ml) was added to heparin-coated wells of heparin binding plate and incubation continued for 2 h at 37 °C. Bound HMGB1 was detected with anti-HMGB1 monoclonal antibody, followed by anti-mouse IgG-HRP. Data are the means ± S.E.M. of 3 wells. $^{**}P<0.01$ *vs.* HMGB1 alone.

TNF-α mRNA compared with the PBS-alone group. TNF-α and VEGF-A_{120} mRNA levels were significantly increased in the group treated with the combination of HMGB1 and heparin compared with groups treated with PBS, heparin, HMGB1 and HRG alone. The addition of HRG suppressed the enhanced expression of TNF-α and VEGF-A_{120} mRNA induced by the combination of HMGB1 and heparin (Fig. 5B).

3.5. Effects of VEGF, HRG and heparin on angiogenesis using matrigel plug assay

We assessed the anti-angiogenic effects of HRG on VEGF-induced angiogenesis using the matrigel plug assay. Ten days after inoculation, the matrigel plugs were recovered. VEGF-A_{165} (250 ng/ml, 6.5 nM), a heparin binding growth factor, alone did not induce angiogenesis (Fig. 6), whereas the combination of VEGF-A_{165} and heparin did induce angiogenesis (Fig. 6). Angiogenesis induced by VEGF-A_{165} and heparin was suppressed by HRG, as in the combination of HMGB1 and heparin. VEGF-A_{121} (185 ng/ml, 6.5 nM) lacking the heparin-binding domain alone and the combination of VEGF-A_{121} and heparin did not induce angiogenesis significantly. These results suggested that heparin has an important role in VEGF-induced angiogenesis.

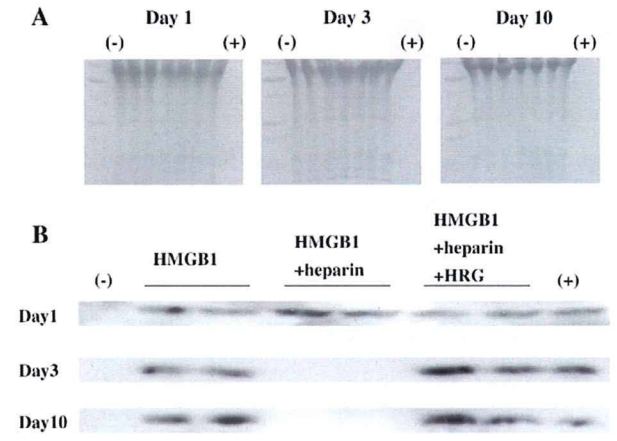

Fig. 4. Determination of HMGB1 levels in matrigel using Western blot analysis matrigel mixture contained PBS, HMGB1, heparin + HMGB1 or heparin + HMGB1 + HRG. After 1, 3 and 10 days, the matrigel plugs were recovered. Matrigel plug homogenate corresponding to 2.5 mg wet weight of matrigel was loaded onto each lane. (A) Ponseau S staining of PVDF membrane. (B) Detection of HMGB1 in matrigel. (−) Negative control, matrigel contains PBS alone. (+) Positive control, recombinant human HMGB1.

4. Discussion

In the previous study, we reported that HMGB1 in complex with heparin induced marked angiogenesis in the matrigel plug assay (Wake et al., 2009). One of the main reasons for heparin dependence of the angiogenic effect of HMGB1 was demonstrated to be due to the diffusibility of HMGB1 and heparin complex from matrigel into surrounding tissue where the proliferation of infiltrating microvasculature occurred (Wake et al., 2009). It was speculated that the restriction of diffusion of HMGB1 alone was ascribed to the binding of HMGB1 to the abundant heparan sulfate proteoglycan structure in matrigel. The other reason may be the resistance of HMGB1 and heparin complex to degradation by proteases (Wake et al., 2009). Collectively, HMGB1 in complex with heparin can diffuse to surrounding matrigel and stimulate vascular endothelial cells without degradation by proteases. Consistent with these findings, HMGB1 in combination with heparin induced the expression of TNF-α and VEGF-A_{120} mRNA. Since it is known that both TNF-α and VEGF-A_{120} have angiogenic activities (Leibovich et al., 1987; Yoshida et al., 1997; Hoeben et al., 2004), the present result implies that HMGB1 release may occur upstream of TNF-α and VEGF-A_{120} production under some *in vivo* conditions. Moreover, VEGF-A_{165}, heparin-binding growth factor, in complex with heparin, induced angiogenesis. This revealed that heparin has an important role in heparin-binding growth factor-induced angiogenesis.

In the present study, HRG completely inhibited the angiogenesis induced by HMGB1 and heparin complex. Because HRG was also reported to interact strongly with heparin (K_d~7 nM) (Lijnen et al., 1983), we examined the competition between HMGB1 and HRG for heparin binding (Fig. 3). The results suggested that HMGB1 and HRG have similar affinity for heparin and are competitive for heparin binding under a constant level of heparin; therefore, it is quite likely that the addition of HRG to matrigel replaced the binding of HMGB1 to heparin, facilitating the trapping of HMGB1 by heparan sulfate proteoglycan in matrigel. This notion was strongly supported by the determination of HMGB1 levels in matrigel under different conditions. Additionally, HRG is known to inhibit the digestion of heparan sulfate by heparanase released from macrophages and mast cells (Freeman and Parish, 1997), thereby inhibiting the de-anchoring of HMGB1 from extracellular matrix (ECM). Parallel and complete inhibitory effects of HRG on both angiogenesis and the expression of TNF-α and VEGF-A_{120} induced by the combination of HMGB1 and heparin strongly suggested that the limitation of HMGB1 diffusion, suppression of TNF-α and VEGF-A_{120} expression and inhibition of angiogenesis were causative and successive events in this matrigel assay system. In the present study, we also demonstrated that HRG inhibited the heparin-dependent effect of VEGF-A_{165} with the heparin-binding domain on angiogenesis. Moreover, it was reported that HRG inhibited the heparin-dependent effect of bFGF on angiogenesis (Juarez et al., 2002; Guan et al., 2004). These findings as a whole suggest that HRG may be a common inhibitor of heparin-binding growth factors.

HMGB1 was reported to be released from necrotic cells. HMGB1 has multiple pro-inflammatory effects on vascular endothelial cells as well as leucocytes. In addition, the present study confirmed the heparin-dependent angiogenic activity of HMGB1; therefore, it is speculated that the release of heparin from mast cells at a certain stage of inflammation may trigger angiogenic activity by de-anchoring the extracellular HMGB1 trapped by heparan sulfate in ECM or on the cell surface. Furthermore, the subsequent exposure of HMGB1–heparin complex to a relatively high concentration of HRG in plasma after canalization will arrest angiogenesis by competing heparin binding. Thus, HRG may also regulate the angiogenic activity of multiple factors, including HMGB1.

It was reported that many types of cancer cells release HMGB1 (Kawahara et al., 1996; Taguchi et al., 2000; Choi et al., 2003; Kuniyasu et al., 2003, 2004) and that mast cells with heparin-containing granules are abundant in the invasive front of tumors (Yoshii et al., 2005; Halin

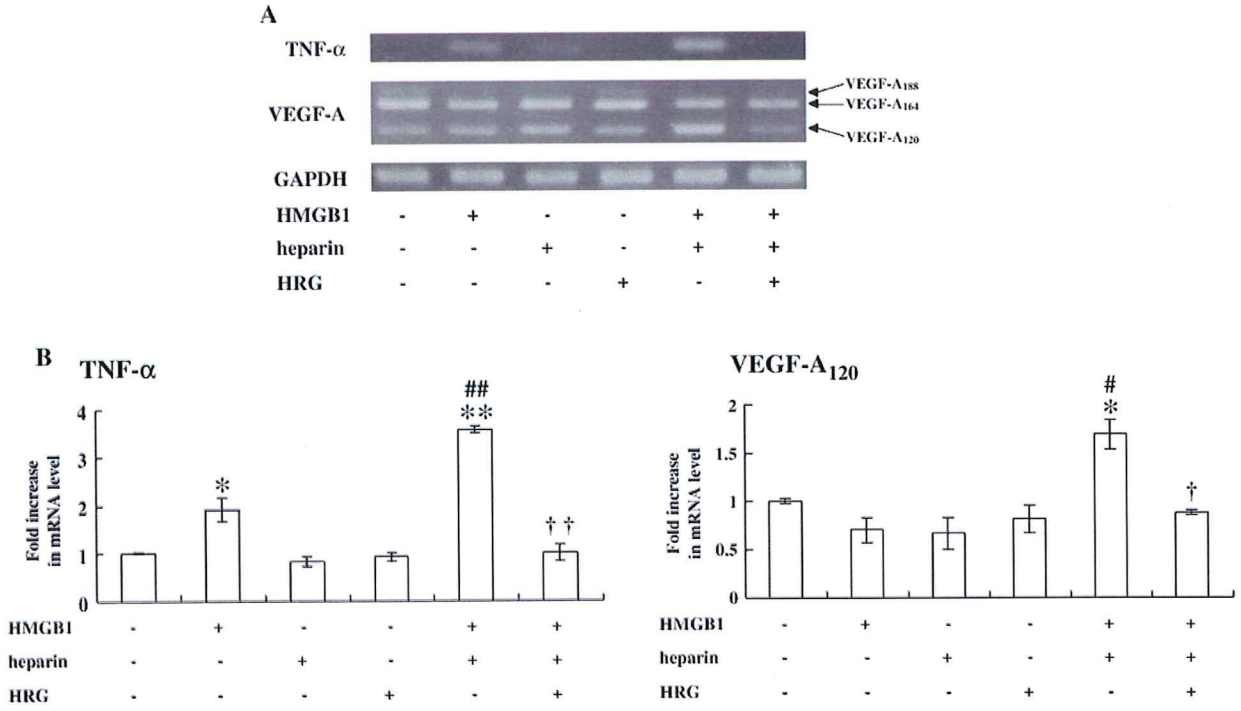

Fig. 5. Expression of mRNAs in mouse skin surrounding matrigel plug. (A) The expression of mRNA in mouse skin surrounding matrigel was determined by RT-PCR. Ten days after inoculation with matrigel, total RNA was extracted from mouse skin surrounding matrigel. Representative results from 3 mice are shown. (B) The expression of TNF-α and VEGF-A_{120} in mouse skin surrounding the matrigel plug was quantified using real-time PCR. The expression of GAPDH was used to normalize cDNA levels. Data are the means ± S.E.M. of 3 animals. $^{*}P<0.05$, $^{**}P<0.01$ *vs.* control group; $^{\#\#}P<0.01$ *vs.* combination of HMGB1 and heparin.

et al., 2009); therefore, it is possible that part of the angiogenic activity of the invasive front of tumors may be ascribed to the action of HMGB1 and heparin complex. HRG not only inhibits VEGF- and bFGF-induced angiogenesis in the presence of heparin but also suppresses tumor growth (Juarez et al., 2002; Doñate et al., 2004; Guan et al., 2004; Olsson et al., 2004). These findings imply that HRG or HRG-derived active

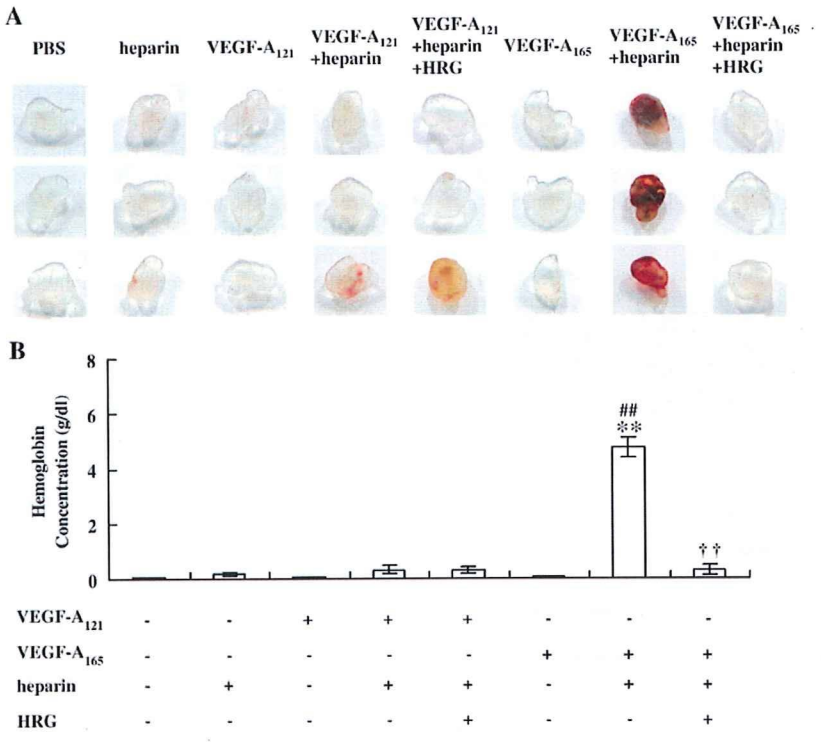

Fig. 6. Effect of HRG on angiogenesis induced by VEGF using matrigel. (A) Matrigel mixture contained VEGF-A_{121}, VEGF-A_{165}, HRG and heparin alone or in combination. Ten days after inoculation, the matrigel plugs were recovered. Each group consisted of 6 mice. (B) Hemoglobin contents in matrigel plugs were determined. Data are the means ± S.E.M. of 6 matrigels. $^{**}P<0.01$ *vs.* PBS control without treatment. $^{\#\#}P<0.01$ *vs.* heparin alone. $^{\dagger\dagger}P<0.01$ *vs.* combination of VEGF-A_{165} and heparin.

domain peptides may have high potential for cancer therapy. Further work is necessary on this issue.

Acknowledgements

This work was supported in part by grants-in-aid for scientific research from the Japan Foundation of Cardiovascular Research to H.W., from the Japan Society for the Promotion of Science (JSPS No. 21390071 and JSPS No. 21659141) to M.N. and (JSPS No. 21590594) to K.L. and from Mitsui Sumitomo Insurance Welfare Foundation to S.M.

References

Burch, M.K., Blackburn, M.N., Morgan, W.T., 1987. Further characterization of the interaction of histidine-rich glycoprotein with heparin: evidence for the binding of two molecules of histidine-rich glycoprotein by high molecular weight heparin and for the involvement of histidine residues in heparin binding. Biochemistry 26, 7477–7482.

Bustin, M., 1999. Regulation of DNA-dependent activities by the functional motifs of the high-mobility-group chromosomal proteins. Mol. Cell. Biol. 19, 5237–5246.

Choi, Y.R., Kim, H., Kang, H.J., Kim, N.G., Kim, J.J., Park, K.S., Paik, Y.K., Kim, H.O., Kim, H., 2003. Overexpression of high mobility group box 1 in gastrointestinal stromal tumors with KIT mutation. Cancer Res. 63, 2188–2193.

Doñate, F., Juarez, J.C., Guan, X., Shipulina, N.V., Plunkett, M.L., Tel-Tsur, Z., Shaw, D.E., Morgan, W.T., Mazar, A.P., 2004. Peptides derived from the histidine–proline domain of the histidine–proline-rich glycoprotein bind to tropomyosin and have antiangiogenic and antitumor activities. Cancer Res. 64, 5812–5817.

Drasin, T., Sahud, M., 1996. Blood-type and age affect human plasma levels of histidine-rich glycoprotein in a large population. Thromb. Res. 84, 179–188.

Freeman, C., Parish, C.R., 1997. A rapid quantitative assay for the detection of mammalian heparanase activity. Biochem. J. 325, 229–237.

Gorgani, N.N., Parish, C.R., Easterbrook, Smith, S.B., Altin, J.G., 1997. Histidine-rich glycoprotein binds to human IgG and C1q and inhibits the formation of insoluble immune complexes. Biochemistry 36, 6653–6662.

Guan, X., Juarez, J.C., Qi, X., Shipulina, N.V., Shaw, D.E., Morgan, W.T., McCrae, K.R., Mazar, A.P., Doñate, F., 2004. Histidine–proline rich glycoprotein (HPRG) binds and transduces anti-angiogenic signals through cell surface tropomyosin on endothelial cells. Thromb. Haemost. 92, 403–412.

Guthans, S.L., Morgan, W.T., 1982. The interaction of zinc, nickel and cadmium with serum albumin and histidine-rich glycoprotein assessed by equilibrium dialysis and immunoadsorbent chromatography. Arch. Biochem. Biophys. 218, 320–328.

Halin, S., Rudolfsson, S.H., Van Rooijen, N., Bergh, A., 2009. Extratumoral macrophages promote tumor and vascular growth in an orthotopic rat prostate tumor model. Neoplasia 11, 177–186.

Hoeben, A., Landuyt, B., Highley, M.S., Wildiers, H., Van Oosterom, A.T., De Bruijn, E.A., 2004. Vascular endothelial growth factor and angiogenesis. Pharmacol. Rev. 56, 549–580.

Juarez, J.C., Guan, X., Shipulina, N.V., Plunkett, M.L., Parry, G.C., Shaw, D.E., Zhang, J.C., Rabbani, S.A., McCrae, K.R., Mazar, A.P., Morgan, W.T., Doñate, F., 2002. Histidine–proline-rich glycoprotein has potent antiangiogenic activity mediated through the histidine–proline-rich domain. Cancer Res. 62, 5344–5350.

Karlsson, S., Pettilä, V., Tenhunen, J., Laru-Sompa, R., Hynninen, M., Ruokonen, E., 2008. HMGB1 as a predictor of organ dysfunction and outcome in patients with severe sepsis. Intensive Care Med. 34, 1046–1053.

Kawahara, N., Tanaka, T., Yokomizo, A., Nanri, H., Ono, M., Wada, M., Kohno, K., Takenaka, K., Sugimachi, K., Kuwano, M., 1996. Enhanced coexpression of thioredoxin and high mobility group protein 1 genes in human hepatocellular carcinoma and the possible association with decreased sensitivity to cisplatin. Cancer Res. 56, 5330–5333.

Kleinman, H.K., McGarvey, M.L., Hassell, J.R., Star, V.L., Cannon, F.B., Laurie, G.W., Martin, G.R., 1986. Basement membrane complexes with biological activity. Biochemistry 25, 312–318.

Koide, T., Foster, D., Yoshitake, S., Davie, E.W., 1986. Amino acid sequence of human histidine-rich glycoprotein derived from the nucleotide sequence of its cDNA. Biochemistry 25, 2220–2225.

Kuniyasu, H., Chihara, Y., Kondo, H., 2003. Differential effects between amphoterin and advanced glycation end products on colon cancer cells. Int. J. Cancer 104, 722–727.

Kuniyasu, H., Sasaki, T., Sasahira, T., Ohmori, H., Takahashi, T., 2004. Depletion of tumor-infiltrating macrophages is associated with amphoterin expression in colon cancer. Pathobiology 71, 129–136.

Leibovich, S.J., Polverini, P.J., Shepard, H.M., Wiseman, D.M., Shively, V., Nuseir, N., 1987. Macrophage-induced angiogenesis is mediated by tumour necrosis factor-alpha. Nature 329, 630–632.

Leung, L.L., Nachman, R.L., Harpel, P.C., 1984. Complex formation of platelet thrombospondin with histidine-rich glycoprotein. J. Clin. Invest. 73, 5–12.

Leung, L.L., 1986. Interaction of histidine-rich glycoprotein with fibrinogen and fibrin. J. Clin. Invest. 77, 1305–1311.

Lijnen, H.R., Hoylaerts, M., Collen, D., 1980. Isolation and characterization of a human plasma protein with affinity for the lysine binding sites in plasminogen. Role in the regulation of fibrinolysis and identification as histidine-rich glycoprotein. J. Biol. Chem. 255, 10214–10222.

Lijnen, H.R., Hoylaerts, M., Collen, D., 1983. Heparin binding properties of human histidine-rich glycoprotein. Mechanism and role in the neutralization of heparin in plasma. J. Biol. Chem. 258, 3803–3808.

Liu, K., Mori, S., Takahashi, H.K., Tomono, Y., Wake, H., Kanke, T., Sato, Y., Hiraga, N., Adachi, N., Yoshino, T., Nishibori, M., 2007. Anti-high mobility group box 1 monoclonal antibody ameliorates brain infarction induced by transient ischemia in rats. FASEB J. 21, 3904–3916.

Mitola, S., Belleri, M., Urbinati, C., Coltrini, D., Sparatore, B., Pedrazzi, M., Melloni, E., Presta, M., 2006. Cutting edge: extracellular high mobility group box-1 protein is a proangiogenic cytokine. J. Immunol. 176, 12–15.

Morgan, W.T., 1981. Interactions of the histidine-rich glycoprotein of serum with metals. Biochemistry 20, 1054–1061.

Morgan, W.T., 1985. The histidine-rich glycoprotein of serum has a domain rich in histidine, proline, and glycine that binds heme and metals. Biochemistry 24, 1496–1501.

Mori, S., Takahashi, H.K., Yamaoka, K., Okamoto, M., Nishibori, M., 2003. High affinity binding of serum histidine-rich glycoprotein to nickel-nitrilotriacetic acid: the application to microquantification. Life Sci. 73, 93–102.

Olsson, A.K., Larsson, H., Dixelius, J., Johansson, I., Lee, C., Oellig, C., Björk, I., Claesson-Welsh, L., 2004. A fragment of histidine-rich glycoprotein is a potent inhibitor of tumor vascularization. Cancer Res. 64, 599–605.

Peterson, C.B., Morgan, W.T., Blackburn, M.N., 1987. Histidine-rich glycoprotein modulation of the anticoagulant activity of heparin. Evidence for a mechanism involving competition with both antithrombin and thrombin for heparin binding. J. Biol. Chem. 262, 7567–7574.

Porto, A., Palumbo, R., Pieroni, M., Aprigliano, G., Chiesa, R., Sanvito, F., Maseri, A., Bianchi, M.E., 2006. Smooth muscle cells in human atherosclerotic plaques secrete and proliferate in response to high mobility group box 1 protein. FASEB J. 20, 2565–2566.

Rylatt, D.B., Sia, D.Y., Mundy, J.P., Parish, C.R., 1981. Autorosette inhibition factor: isolation and properties of the human plasma protein. Eur. J. Biochem. 119, 641–646.

Scaffidi, P., Misteli, T., Bianchi, M.E., 2002. Release of chromatin protein HMGB1 by necrotic cells triggers inflammation. Nature 418, 191–195.

Schlueter, C., Weber, H., Meyer, B., Rogalla, P., Röser, K., Hauke, S., Bullerdiek, J., 2005. Angiogenetic signaling through hypoxia: HMGB1: an angiogenetic switch molecule. Am. J. Pathol. 166, 1259–1263.

Silverstein, R.L., Leung, L.L., Harpel, P.C., Nachman, R.L., 1985. Platelet thrombospondin forms a trimolecular complex with plasminogen and histidine-rich glycoprotein. J. Clin. Invest. 75, 2065–2073.

Taguchi, A., Blood, D.C., del Toro, G., Canet, A., Lee, D.C., Qu, W., Tanji, N., Lu, Y., Lalla, E., Fu, C., Hofmann, M.A., Kislinger, T., Ingram, M., Lu, A., Tanaka, H., Hori, O., Ogawa, S., Stern, D.M., Schmidt, A.M., 2000. Blockade of RAGE-amphoterin signalling suppresses tumour growth and metastases. Nature 405, 354–360.

Taniguchi, N., Kawahara, K., Yone, K., Hashiguchi, T., Yamakuchi, M., Goto, M., Inoue, K., Yamada, S., Ijiri, K., Matsunaga, S., Takajima, T., Komiya, S., Maruyama, I., 2003. High mobility group box chromosomal protein 1 plays a role in the pathogenesis of rheumatoid arthritis as a novel cytokine. Arthritis Rheum. 48, 971–981.

Towbin, H., Staehelin, T., Gordon, J., 1979. Electrophoretic transfer of proteins from polyacrylamide gels to nitrocellulose sheets: procedure and some applications. Proc. Natl. Acad. Sci. U. S. A. 76, 4350–4354.

Wake, H., Mori, S., Liu, K., Takahashi, H.K., Nishibori, M., 2009. High mobility group box 1 complexed with heparin induced angiogenesis in matrigel plug assay. Acta Med. Okayama. 63, 249–262.

Wang, H., Bloom, O., Zhang, M., Vishnubhakat, J.M., Ombrellino, M., Che, J., Frazier, A., Yang, H., Ivanova, S., Borovikova, L., Manogue, K.R., Faist, E., Abraham, E., Andersson, J., Andersson, U., Molina, P.E., Abumrad, N.N., Sama, A., Tracey, K.J., 1999. HMG-1 as a late mediator of endotoxin lethality in mice. Science 285, 248–251.

Wang, H., Yang, H., Czura, C.J., Sama, A.E., Tracey, K.J., 2001. HMGB1 as a late mediator of lethal systemic inflammation. Am. J. Respir. Crit. Care Med. 164, 1768–1773.

Yoshida, S., Ono, M., Shono, T., Izumi, H., Ishibashi, T., Suzuki, H., Kuwano, M., 1997. Involvement of interleukin-8, vascular endothelial growth factor, and basic fibroblast growth factor in tumor necrosis factor alpha-dependent angiogenesis. Mol. Cell. Biol. 17, 4015–4023.

Yoshii, M., Jikuhara, A., Mori, S., Iwagaki, H., Takahashi, H.K., Nishibori, M., Tanaka, N., 2005. Mast cell tryptase stimulates DLD-1 carcinoma through prostaglandin- and MAP kinase-dependent manners. J. Pharmacol. Sci. 98, 450–458.

Yuan, F., Gu, L., Guo, S., Wang, C., Li, G.M., 2004. Evidence for involvement of HMGB1 protein in human DNA mismatch repair. J. Biol. Chem. 279, 20935–20940.

0022-3565/09/3312-656–670$20.00
THE JOURNAL OF PHARMACOLOGY AND EXPERIMENTAL THERAPEUTICS
Copyright © 2009 by The American Society for Pharmacology and Experimental Therapeutics
JPET 331:656–670, 2009

Vol. 331, No. 2
157594/3527560
Printed in U.S.A.

Prostaglandin E_2 Inhibits Advanced Glycation End Product-Induced Adhesion Molecule Expression, Cytokine Production, and Lymphocyte Proliferation in Human Peripheral Blood Mononuclear Cells

Hideo Kohka Takahashi, Keyue Liu, Hidenori Wake, Shuji Mori, Jiyong Zhang, Rui Liu, Tadashi Yoshino, and Masahiro Nishibori

Departments of Pharmacology (H.K.T., K.L., H.W., J.Z., R.L., M.N.) and Pathology (T.Y.), Okayama University Graduate School of Medicine, Dentistry, and Pharmaceutical Sciences, Okayama, Japan; and Department of Pharmacy, Shujitsu University, Okayama, Japan (S.M.)

Received June 11, 2009; accepted August 20, 2009

ABSTRACT

Advanced glycation end product (AGE) subtypes, proteins or lipids that become glycated after exposure to sugars, induce complications in diabetes. Among the various AGE subtypes, glyceraldehyde-derived AGE (AGE-2) and glycolaldehyde-derived AGE (AGE-3) have been indicated to play roles in inflammation in diabetic patients. The engagement of AGEs and receptor for AGEs activates monocytes. Because the engagement of intercellular adhesion molecule-1 (ICAM-1), B7.1, B7.2, and CD40 on monocytes with their ligands on T cells plays roles in cytokine production, we investigated the effects of AGE-2 and AGE-3 on the expressions of ICAM-1, B7.1, B7.2, and CD40 on monocytes, the production of interferon γ and tumor necrosis factor α, and the lymphocyte proliferation in human peripheral blood mononuclear cells and their modulation by prostaglandin E_2 (PGE_2). AGE-2 and AGE-3 induced the expressions of adhesion molecule, the cytokine production, and the lymphocyte proliferation. PGE_2 concentration-dependently inhibited the actions of AGE-2 and AGE-3. The effects of PGE_2 were mimicked by an E-prostanoid $(EP)_2$-receptor agonist, 11,15-*O*-dimethyl prostaglandin E_2 (ONO-AE1-259-01), and an EP_4 receptor agonist, 16-(3-methoxymethyl)phenyl-ω-tetranor-3,7-dithia prostaglandin E_1 (ONO-AE1-329). An EP_2-receptor antagonist, 6-isopropoxy-9-oxaxanthene-2-carboxylic acid (AH6809), and an EP_4-receptor antagonist, (4*Z*)-7-[(rel-1*S*,2*S*,5*R*)-5-(1,1′-biphenyl-4-yl)methoxy)-2-(4-morpholinyl)-3-oxocyclopentyl]-4-heptenoic acid (AH23848), inhibited the actions of PGE_2. The stimulation of EP_2 and EP_4 receptors is reported to increase cAMP levels. The effects of PGE_2 were reversed by a protein kinase A (PKA) inhibitor, H89, and mimicked by a dibutyryl cAMP and an adenylate cyclase activator, forskolin. These results as a whole indicated that PGE_2 inhibited the actions of AGE-2 and AGE-3 via EP_2/EP_4 receptors and the cAMP/PKA pathway.

It is known that sugars, including glucose, fructose, and triose, react with amino groups of proteins nonenzymatically, leading to the formation of advanced glycation end product (AGE) (Brownlee et al., 1988). AGEs, a heterogeneous group of complex structures, form nonenzymatically when reducing sugars react with free amino groups on proteins, lipids, or nucleic acids. The formation and accumulation of AGEs occur at an accelerated rate in diabetic patients and may participate in the pathogenesis of diabetic micro- and macrovascular complications (Bierhaus et

This work was supported in part by the Japan Society for the Promotion of Science [Grants 18590509, 20590539, 17659159, 19659061, 21659141, 21390071, and 215905694]; the Scientific Research from Ministry of Health, Labor, and Welfare of Japan; and the Takeda Science Foundation.
Article, publication date, and citation information can be found at http://jpet.aspetjournals.org.
doi:10.1124/jpet.109.157594.

ABBREVIATIONS: AGE, advanced glycation end product; RAGE, receptor for advanced glycation end product; NF-κB, nuclear factor κB; TNF, tumor necrosis factor; IL, interleukin; ICAM, intercellular adhesion molecule; IFN, interferon; PBMC, peripheral blood mononuclear cell; PGE_2, prostaglandin E_2; COX, cyclooxygenase; AH6809, 6-isopropoxy-9-oxaxanthene-2-carboxylic acid; AH23848, [1α(*Z* BSA, bovine serum albumin; dbcAMP, dibutyryl cAMP; FITC, fluorescein isothiocyanate; mAb, monoclonal antibody; ELISA, enzyme-linked immunosorbent assay; sRAGE, soluble form of RAGE; PKA, protein kinase A; NS-398, *N*-[2-(cyclohexyloxyl)-4-nitrophenyl]-methane sulfonamide; EP, E-prostanoid; ONO-AE1-259-01, 11,15-O-dimethyl prostaglandin E_2; ONO-AE1-329, 16-(3-methoxymethyl)phenyl-ω-tetranor-3,7-dithia prostaglandin E_1; AH23848, (4Z)-7-[(rel-1S,2S,5R)-5-(1,1′-biphenyl-4-yl)methoxy)-2-(4-morpholinyl)-3-oxocyclopentyl]-4-heptenoic acid; ONO-DI-004, 17S-2,5-ethano-6-oxo-17,20-dimethyl prostaglandin E_1; ONO-AE-248, 16S-9-deoxy-9β-chloro-15-deoxy-16-hydroxy-17,17-trimethylene-19,20-didehydro prostaglandin F_2.

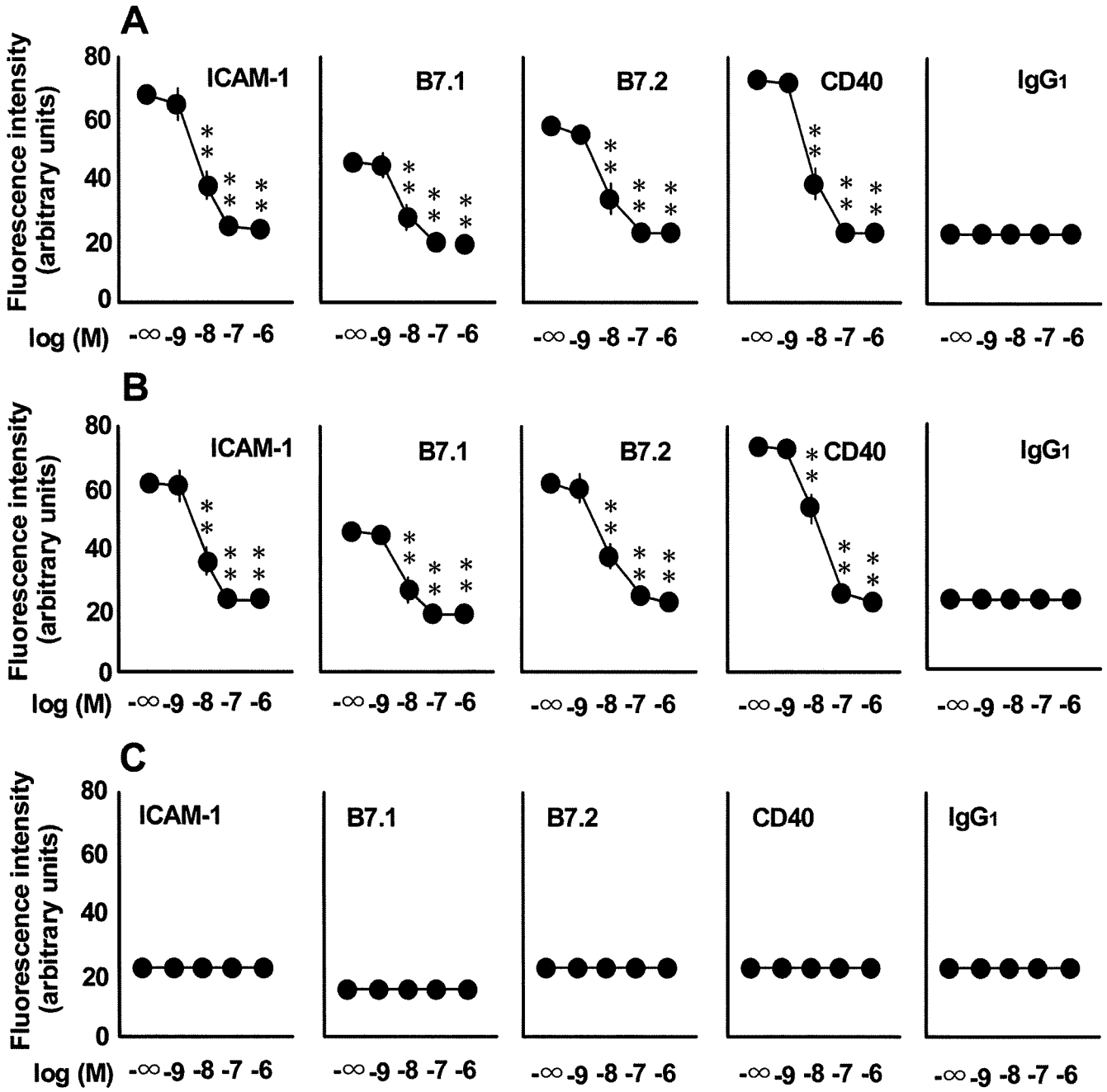

Fig. 1. The effects of PGE_2 on AGE-2- and AGE-3-induced expressions of ICAM-1, B7.1, B7.2, and CD40 on monocytes PBMC at 1×10^6 cells/ml were incubated with PGE_2 at increasing concentrations from 1 nM to 1 μM in the presence of AGE-2 (A), AGE-3 (B), and BSA (C) at 100 μg/ml for 24 h. The expressions of ICAM-1, B7.1, B7.2, and CD40 on monocytes were determined by flow cytometry. Isotype-matched control represents FITC-conjugated IgG1. The results are expressed as the means ± S.E.M. of five donors with triplicate determinations. **, $P < 0.01$ compared with the value for AGE-2 and AGE-3. When an error bar was within a symbol, the bar was omitted.

al., 1998; Fukami et al., 2004). It provided direct immunochemical evidence of the existence of four distinct AGE structures, including AGE-2, AGE-3, AGE-4, and AGE-5, within AGE-modified proteins and peptides (Takeuchi and Yamagishi, 2004). Among the various subtypes of AGE, it has been shown that glyceraldehyde-derived AGE (AGE-2) and glycolaldehyde-derived AGE (AGE-3) are the main AGE structures detectable in the serum of diabetic patients. Toxic AGE structures, AGE-2 and AGE-3, have diverse biological activities on vascular wall cells, mesangial cells, Schwann cells, malignant melanoma cells, and cortical neurons (Okamoto et al., 2002; Yamagishi et al., 2002). AGE-2 plays roles in the development of atherosclerosis (Takeuchi et al., 2000). The interaction between AGEs and the receptor for AGEs (RAGE) perturbs a variety of vascular homeostatic functions and thus may contribute to diabetic vasculopathy (Schmidt et al., 1994; Wautier et al., 1996; Park et al., 1998). AGEs and RAGE are reported to be detected in atherosclerotic plaque of diabetic patients (Cuccurullo et al., 2006). A recent study

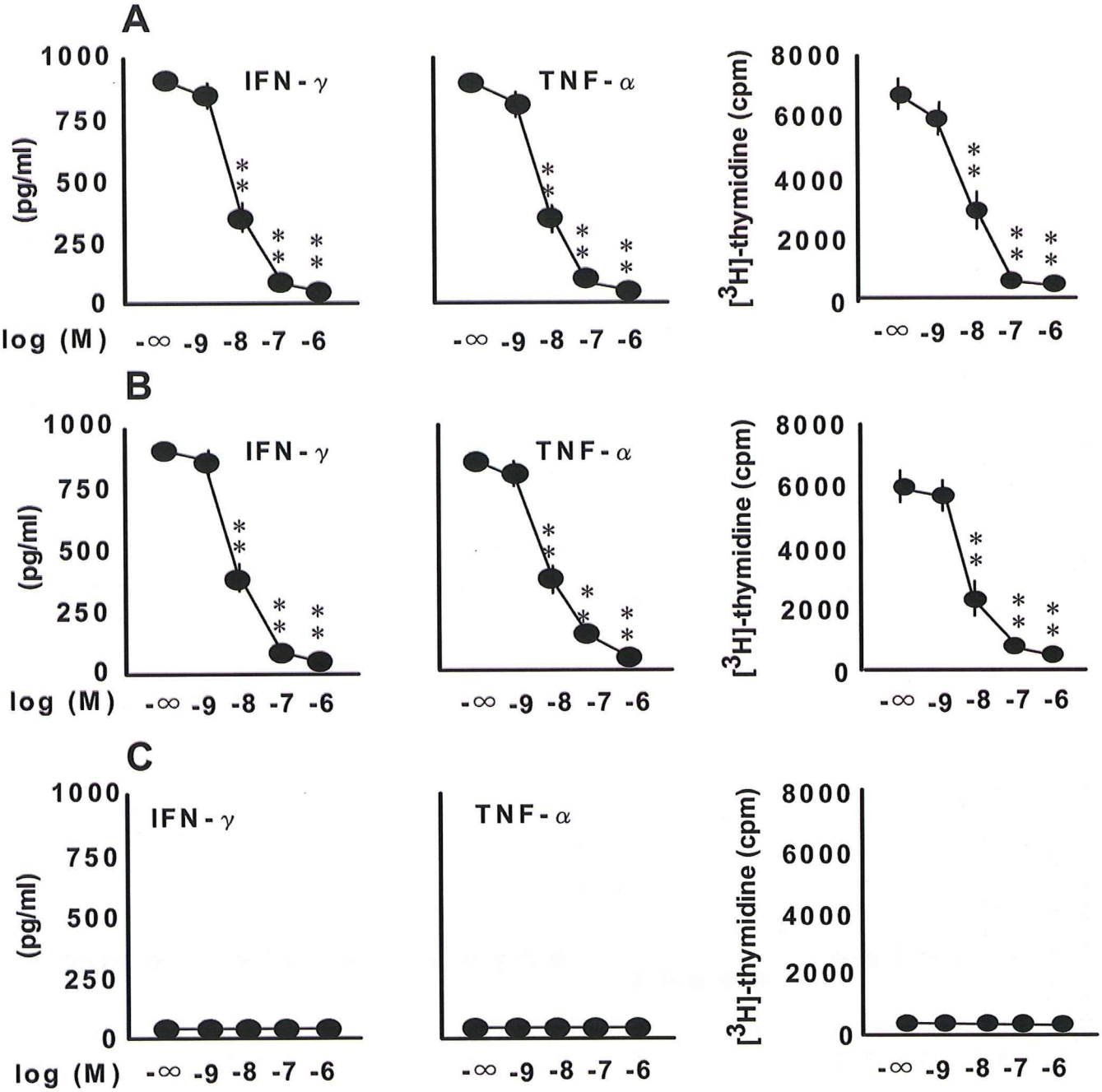

Fig. 2. The effects of PGE_2 on AGE-2- and AGE-3-induced production of IFN-γ and TNF-α and the lymphocyte proliferation in PBMC. The effect of PGE_2 at increasing concentrations from 1 nM to 1 μM in the presence of AGE-2 (A), AGE-3 (B), and BSA (C) at 100 μg/ml on IFN-γ and TNF-α concentrations in conditioned media was determined by ELISA. The lymphocyte proliferation was determined by [^{3}H]thymidine uptake as described under *Materials and Methods*. The results are expressed as the means ± S.E.M. of five donors with triplicate determinations. **, $P < 0.01$ compared with the value for AGE-2 and AGE-3. When an error bar was within a symbol, the bar was omitted.

reported that RAGE expression is associated with apoptotic smooth muscle cells and macrophages, suggesting that RAGE may promote plaque destabilization (Burke et al., 2004). It is reported that AGE-modified proteins can induce various proinflammatory and procoagulant cellular responses resulting from nuclear factor κB (NF-κB) activation (Yan et al., 1994), including the expression of vascular cell adhesion molecule-1, tumor necrosis factor (TNF)-α, interleukin (IL)-6, and tissue factor (Schmidt et al., 1994, 1995; Miyata et al., 1996; Bierhaus et al., 1997; Hofmann et al., 1999).

Microinflammation plays roles in the pathogenesis of diabetic vascular complications. It is reported that diabetes has more macrophage and T-cell infiltration in atherosclerotic plaques (Burke et al., 2004). Activation of monocytes/macrophages and T cells induces the progression of inflammatory atherosclerotic plaques (Stoll and Bendszus, 2006). The enhanced expression of adhesion molecule, including intercel-

TABLE 1
The IC_{50} values for the inhibitory effect of PGE_2 and $EP_{2/4}$ receptor agonists in the presence of AGE-2 and AGE-3
The results are expressed as the means ± S.E.M. of five donors with triplicate determinations.

	ICAM-1	B7.1	B7.2	CD40	TNF-α	IFN-γ	Proliferation
				nM			
AGE-2							
PGE_2	7 ± 0.2	7 ± 0.2	8 ± 0.3	8 ± 0.2	7 ± 0.2	8 ± 0.3	7 ± 0.3
ONO-AE1-259-01	9 ± 0.2	10 ± 0.1	10 ± 0.1	8 ± 0.3	7 ± 0.2	8 ± 0.2	7 ± 0.2
ONO-AE1-329	9 ± 0.2	10 ± 0.2	10 ± 0.1	10 ± 0.2	10 ± 0.2	10 ± 0.2	10 ± 0.3
AGE-3							
PGE_2	8 ± 0.3	8 ± 0.1	10 ± 0.2	15 ± 0.3	8 ± 0.3	8 ± 0.1	7 ± 0.4
ONO-AE1-259-01	8 ± 0.2	10 ± 0.1	10 ± 0.2	8 ± 0.2	7 ± 0.2	8 ± 0.2	8 ± 0.2
ONO-AE1-329	9 ± 0.2	10 ± 0.1	10 ± 0.2	10 ± 0.1	10 ± 0.3	10 ± 0.1	10 ± 0.2

lular adhesion molecule (ICAM)-1, B7, and CD40, on monocytes results in the activation of T cells (Durie et al., 1994; Ranger et al., 1996; Camacho et al., 2001). We also found that cell-to-cell interactions were brought about via the engagement between ICAM-1, B7.1, B7.2, and CD40 on monocytes and their ligands; lymphocyte function-associated antigen 1, CD28, and CD40 ligand on T cells were involved in T-cell activation, inducing the production of TNF-α and interferon (IFN)-γ in peripheral blood mononuclear cells (PBMC) (Takahashi et al., 2003). Blockade of the engagement of adhesion molecules by antibodies against ICAM-1, B7.1, B7.2, and CD40 reduced cytokine production in PBMC. In a previous study, we found that AGE-2 and AGE-3, but not AGE-4 and AGE-5, induced the expressions of ICAM-1, B7.1, B7.2, and CD40 on monocytes, the production of IFN-γ and TNF-α, and the lymphocyte proliferation in PBMC (Takahashi et al., 2009; Wake et al., 2009). We suggested that the activation of T cells by the enhancement of adhesion molecule expression on monocytes might result in the development of diabetic microangiopathy.

Prostaglandin E_2 (PGE_2), one of the major products of cyclooxygenase (COX)-initiated arachidonic acid metabolite released from monocytes, primes naive human T cells for enhanced production of anti-inflammatory cytokines and the inhibition of proinflammatory cytokines through COX-2 (Coleman et al., 1994; Hempel et al., 1994). There are four subtypes of PGE_2 receptors: prostanoid EP_1, EP_2, EP_3, and EP_4 receptors (Coleman et al., 1994). Activation of EP_2 and EP_4 receptors leads to an increase in cAMP levels (Coleman et al., 1994). However, little is known about the effect of PGE_2 on the AGE-2- and AGE-3-induced adhesion molecule expressions on monocytes. Therefore, we examined the effect of PGE_2 on AGE-2- and AGE-3-induced expressions of ICAM-1, B7.1, B7.2, and CD40 on monocytes, the production of IFN-γ and TNF-α, and the lymphocyte proliferation in PBMC.

Materials and Methods

Reagents and Drugs. PGE_2, AH6809, and AH23848 were purchased from Sigma-Aldrich (St. Louis, MO). ONO-D1-004, ONO-AE1-259-01, ONO-AE-248, ONO-AE1-329, and 11-deoxy-PGE_1 were provided by Ono Pharmaceutical Co. Ltd. (Tokyo, Japan). Glyceraldehyde-derived AGE (AGE-2) and glycolaldehyde-derived AGE (AGE-3) were prepared as described previously (Cuccurullo et al., 2006). In brief, AGE-bovine serum albumin (BSA) was prepared by incubating BSA at 50 mg/ml (Sigma-Aldrich) in $NaPO_4$ buffer (0.2 M, pH 7.4) with D-glyceraldehyde (AGE-2) at 0.2 M and D-glycolaldehyde (AGE-3) at 0.2 M (Wako, Tokyo, Japan) at 37°C for 7 days in the presence of 1.5 mM phenylmethylsulfonyl fluoride, 1 mM EDTA, and 1.0×10^5 U/l penicillin under endotoxin-free conditions. Dibutyryl cAMP (dbcAMP) and forskolin were purchased from Wako. H89 was purchased from Sigma-Aldrich. For flow cytometric analysis, a fluorescein isothiocyanate (FITC)-conjugated mouse IgG1 monoclonal antibody (mAb) against ICAM-1/CD54 was purchased from Dako Denmark A/S (Glostrup, Denmark). FITC-conjugated mouse IgG1 mAbs against B7.2 and CD40 were purchased from BD Pharmingen (San Diego, CA), and an FITC-conjugated IgG1 isotype-matched control was obtained from Sigma-Aldrich.

Isolation of PBMC and Monocytes. Normal human PBMCs were obtained from 10 healthy volunteers after acquiring institutional review board approval (Okayama University Institutional Review Board Number 106). Samples of 20 to 50 ml of peripheral blood were withdrawn from a forearm vein, after which PBMCs were prepared, and monocytes isolated from PBMC were separated by counterflow centrifugal elutriation as described previously (Takahashi et al., 2003). The PBMC and monocytes were then suspended at a final concentration of 1×10^6 cells/ml in the medium as described previously (Takahashi et al., 2003).

Flow Cytometric Analysis. Changes in the expression of human leukocyte antigens ICAM-1, B7.1, B7.2, and CD40 on monocytes were examined by multicolor flow cytometry using a combination of anti-CD14 Ab with anti-ICAM-1, anti-B7.1, anti-B7.2, or anti-CD40 Ab. PBMCs at 1×10^6 cells/ml were incubated for 24 h. Cultured cells at 5×10^5 cells/ml were prepared for flow cytometric analysis as previously described (Takahashi et al., 2003) and analyzed with a FACSCalibur (BD Biosciences, San Jose, CA). The data were processed using the CellQuest program (BD Biosciences).

Cytokine Assay. PBMCs at 1×10^6 cells/ml were used to analyze IFN-γ and TNF-α production. After culturing for 24 h at 37°C in a 5% CO_2/air mixture, cell-free supernatant was assayed for IFN-γ and TNF-α protein by enzyme-linked immunosorbent assay (ELISA) using the multiple Abs sandwich principle (R&D Systems, Minneapolis, MN). The detection limits of ELISA for IFN-γ and TNF-α were 10 pg/ml.

Proliferation Assay. PBMCs were treated with various conditions. Cultures were incubated for 48 h, during which they were pulsed with [^{3}H]thymidine (3 · 3 Ci/well) for the final 16 h. Cells were then divided into 96-well microplates, 200 μl/well, resulting in 1 μCi [^{3}H]thymidine per well, and harvested by the Micro-Mate 196 Cell Harvester (PerkinElmer Life and Analytical Sciences, Waltham, MA). Thymidine incorporation was measured by a beta-counter (Matrix 9600; PerkinElmer Life and Analytical Sciences).

Measurement of cAMP Production in Monocytes. Monocytes at 1×10^6 cells/ml were incubated at 37°C in a 5% CO_2/air mixture under different conditions. After the indicated periods, cells at 2×10^5 cells/200 μl/well were supplemented with trichloroacetic acid to a final concentration of 5% and 3-isobutyl-1-methylxanthine, an inhibitor of phosphodiesterase, at 100 μM and frozen at −80°C. Frozen samples were subsequently sonicated and assayed for cAMP using a cAMP enzyme immunoassay kit (Cayman Chemical, Ann

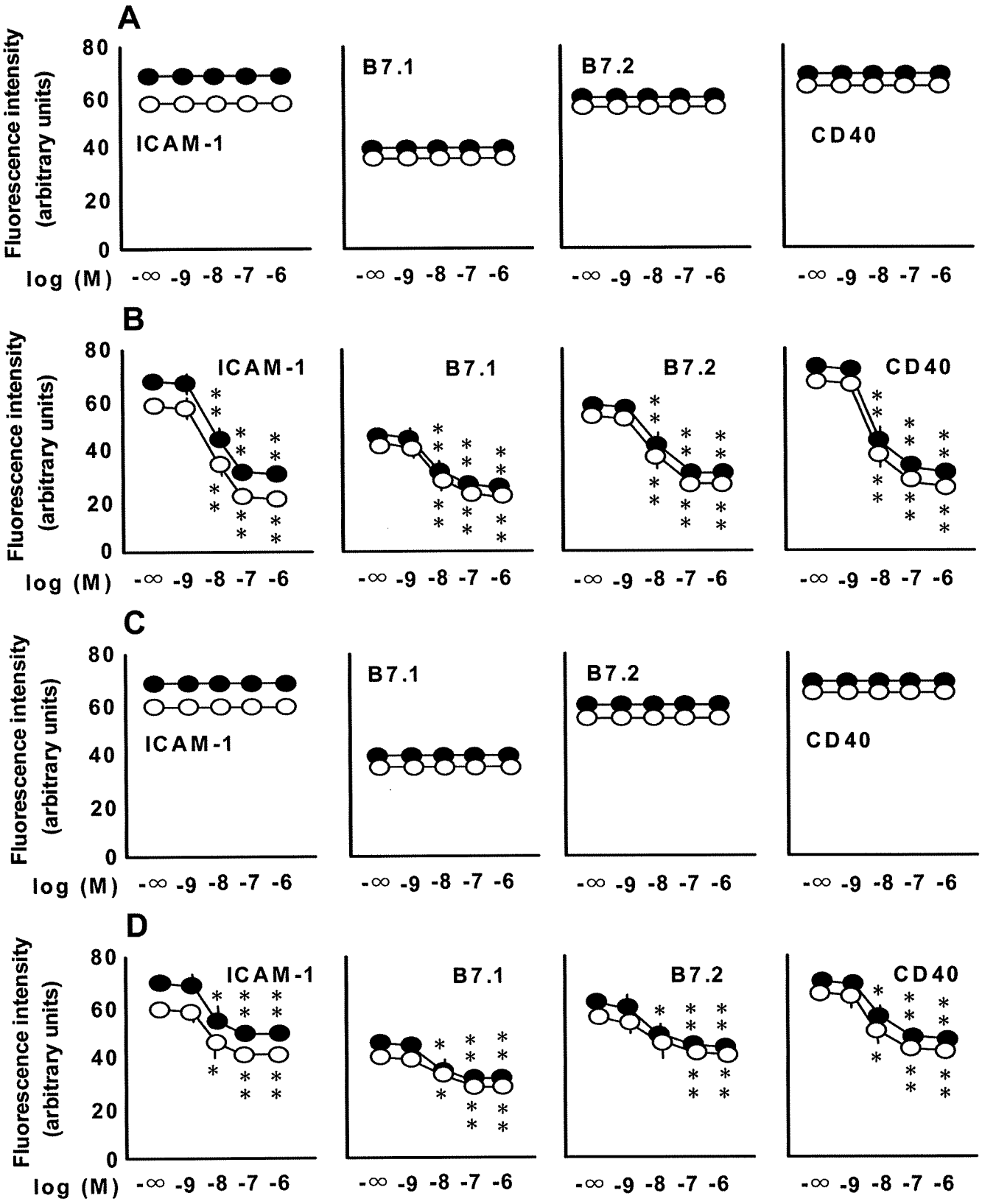

Fig. 3. The effect of prostanoid receptor agonists on AGE-2- and AGE-3-induced expressions of ICAM-1, B7.1, B7.2, and CD40 PBMC at 1×10^6 cells/ml was incubated with the EP_1 receptor agonist, ONO-D1-004 (A), the EP_2 receptor agonist, ONO-AE1-259-01 (B), the EP_3 receptor agonist, ONO-AE-248 (C), and the EP_4-receptor agonist, ONO-AE1-329 (D), at increasing concentrations from 1 nM to 1 μM in the presence of AGE-2 (filled circles; ●) and AGE-3 (open circles; ○) at 100 μg/ml for 24 h. The expressions of ICAM-1, B7.1, B7.2, and CD40 on monocytes were determined by flow cytometry. The results are expressed as the means ± S.E.M. of five donors with triplicate determinations. *, $P < 0.05$, **, $P < 0.01$ compared with the value for AGE-2 and AGE-3. When an error bar was within a symbol, the bar was omitted.

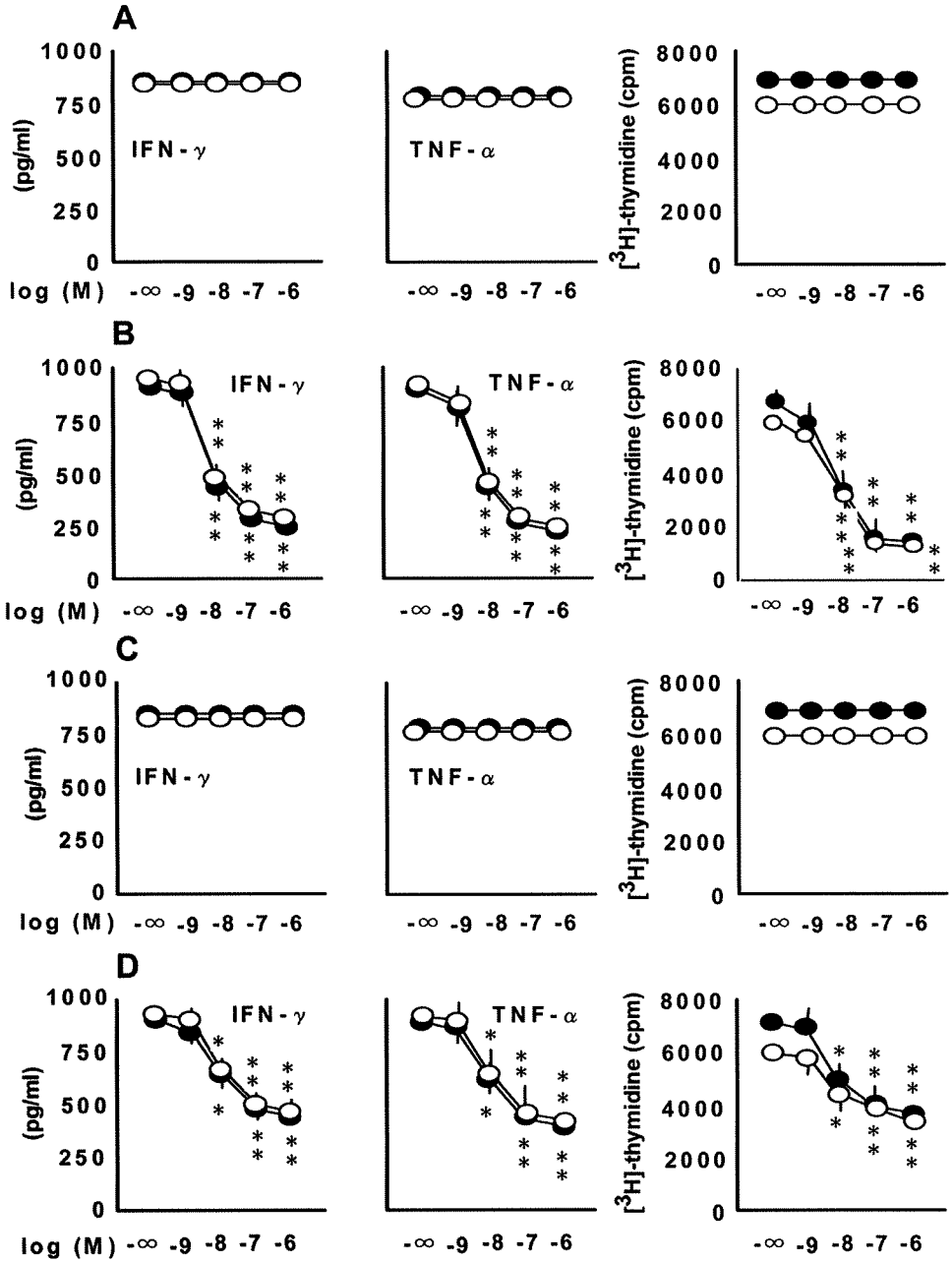

Fig. 4. The effect of prostanoid receptor agonists on AGE-2- and AGE-3-induced production of IFN-γ and TNF-α and the lymphocyte proliferation PBMC at 1×10^6 cells/ml were incubated with the EP_1 receptor agonist, ONO-D1-004 (A), the EP_2 receptor agonist, ONO-AE1-259-01 (B), the EP_3 receptor agonist, ONO-AE-248 (C), and the EP_4 receptor agonist, ONO-AE1-329 (D), at increasing concentrations from 1 nM to 1 μM in the presence of AGE-2 (filled circles; ●) and AGE-3 (open circles; ○) at 100 μg/ml for 24 h. IFN-γ and TNF-α concentrations in conditioned media were determined by ELISA. The lymphocyte proliferation was determined by [^{3}H]thymidine uptake as described under *Materials and Methods*. The results are expressed as the means ± S.E.M. of five donors with triplicate determinations. *, $P < 0.05$, **, $P < 0.01$ compared with the values for AGE-2 and AGE-3. When an error bar was within a symbol, the bar was omitted.

Arbor, MI) according to the manufacturer's instructions, for which no acetylation procedures were performed.

Statistical Examination. Statistical significance was evaluated using analysis of variance followed by Dunnett's test. A probability value of less than 0.05 was considered to indicate statistical significance. The results were expressed as the means ± S.E.M. of triplicate findings from five donors.

Results

Effects of PGE_2 on AGE-2- and AGE-3-Induced Expressions of ICAM-1, B7.1, B7.2, and CD40 on Monocytes, the Production of IFN-γ and TNF-α, and the Lymphocyte Proliferation in PBMC. In the previous study, to evaluate the binding of AGE subtypes to RAGE, we established an in vitro assay by using the immobilized AGE subspecies and the His-tagged soluble form of RAGE (sRAGE) protein (Takahashi et al., 2009). AGE-2 and AGE-3 showed relatively high affinity binding for sRAGE, whereas AGE-4 and AGE-5 showed moderate affinity for sRAGE. The appropriate incubation time and concentration of AGEs were determined according to the study (Takahashi et al., 2009; Wake et al., 2009). AGE-2 and AGE-3 at 100 μg/ml significantly induced the expressions of ICAM-1, B7.1, B7.2, and CD40, the production of IFN-γ and TNF-α, and the proliferation at 16 h and thereafter up to 24 and 48 h. Moreover, the effects of AGE-2 and AGE-3 at concentrations ranging from 100 ng/ml to 100 μg/ml for 24 h were determined. AGE-2 and AGE-3 at 10 and 100 μg/ml significantly induced the expressions of adhesion molecule, the cytokine production, and the lymphocyte proliferation.

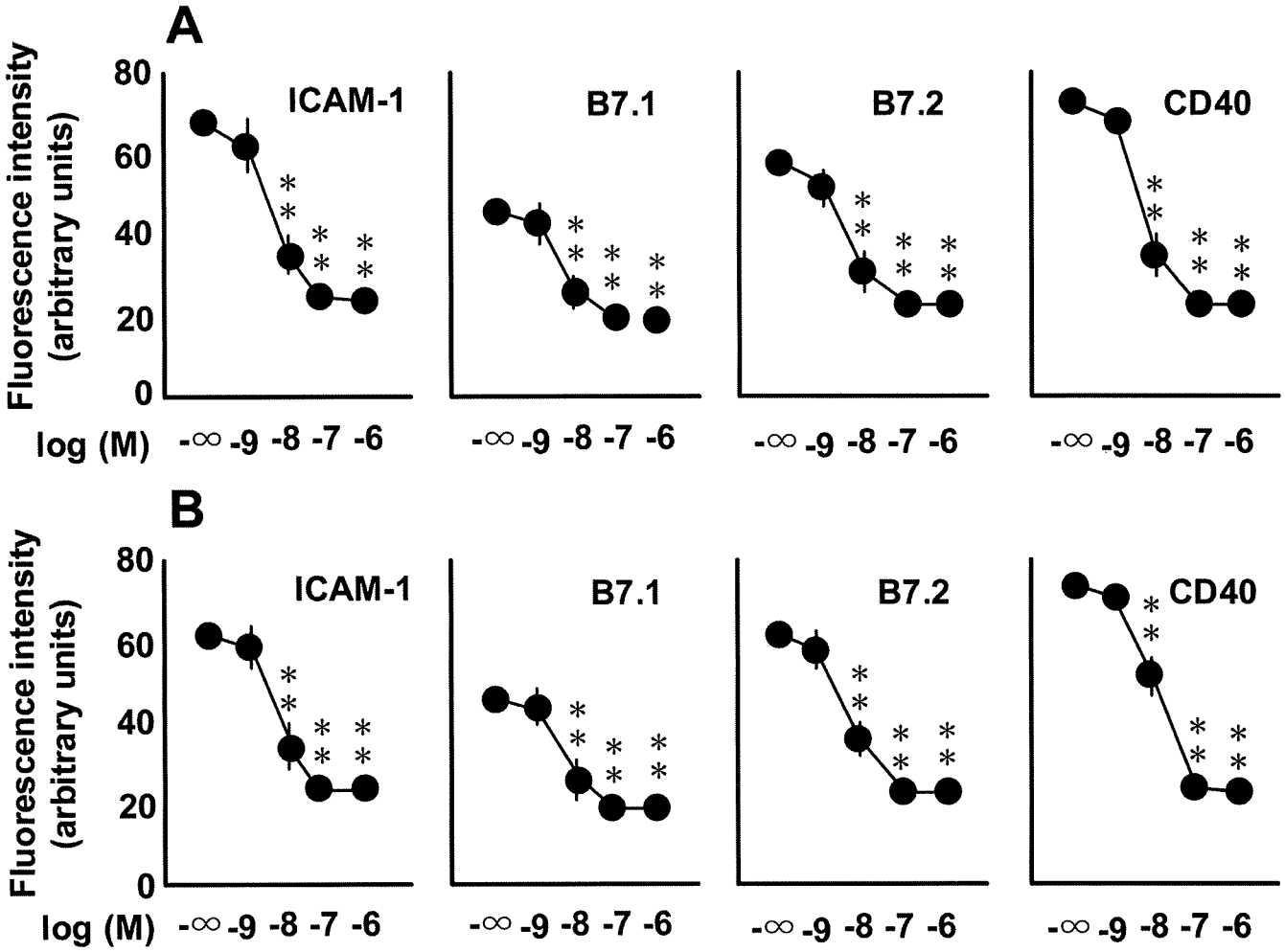

Fig. 5. The effects of 11-deoxy-PGE_1 on AGE-2- and AGE-3-induced ICAM-1, B7.1, B7.2, and CD40 expressions on human monocytes. PBMCs at 1×10^6 cells/ml were incubated with increasing concentrations of the EP_2/EP_4 receptor agonist, 11-deoxy-PGE_1 at increasing concentrations from 1 nM to 1 μM in the presence of AGE-2 (A) and AGE-3 (B) at 100 μg/ml for 24 h. The expressions of ICAM-1, B7.1, B7.2, and CD40 on monocytes were determined by flow cytometry. The results are expressed as the means ± S.E.M. of five donors with triplicate determinations. **, $P < 0.01$ compared with the values for AGE-2 and AGE-3. When an error bar was within a symbol, the bar was omitted.

As shown in Figs. 1 and 2, we established the effect of PGE_2 at concentrations ranging from 1 nM to 1 μM on the expressions of ICAM-1, B7.1, B7.2, and CD40 and its affect on the production of IFN-γ and TNF-α and the lymphocyte proliferation in the presence of AGE-2 and AGE-3 at 100 μg/ml. PGE_2 concentration-dependently inhibited AGE-2- and AGE-3-induced expressions of ICAM-1, B7.1, B7.2, and CD40, the production of IFN-γ and TNF-α, and the lymphocyte proliferation. The IC_{50} values for the inhibitory effect of PGE_2 on the expressions of ICAM-1, B7.1, B7.2, and CD40 and its affect on the production of IFN-γ and TNF-α and the lymphocyte proliferation in the presence of AGE-2 and AGE-3 are shown in Table 1. Moreover, we found that PGE_2 had no effect on the adhesion molecule expression and cytokine production in the presence of AGE-4 and AGE-5 (data not shown).

Involvement of Prostanoid EP_2 and EP_4 Receptors in the Actions of PGE_2. To determine the involvement of PGE_2 receptor subtypes in the effects of PGE_2 on the expressions of ICAM-1, B7.1, B7.2, and CD40, the production of IFN-γ and TNF-α, and the lymphocyte proliferation, the effects of an EP_1 receptor agonist, ONO-D1-004 (Suzawa et al., 2000; Noguchi et al., 2001), an EP_2 receptor agonist, ONO-AE1-259-01 (Suzawa et al., 2000; Noguchi et al., 2001), an EP_3 receptor agonist, ONO-AE-248 (Suzawa et al., 2000; Noguchi et al., 2001), and an EP_4 receptor agonist, ONO-AE1-329 (Suzawa et al., 2000; Noguchi et al., 2001), at concentrations ranging from 1 nM to 1 μM, on the adhesion molecule expression, the cytokine production, and the lymphocyte proliferation in the presence of AGE-2 and AGE-3 at 100 μM were determined (Figs. 3 and 4). The IC_{50} values for the inhibitory effect of ONO-AE1-259-01 and ONO-AE1-329 on the expressions of ICAM-1, B7.1, B7.2, and CD40 and its affect on the production of IFN-γ and TNF-α and the lymphocyte proliferation in the presence of AGE-2 and AGE-3 were shown in Table 1. It is apparent that the EP_2 and EP_4 receptor agonists concentration-dependently inhibited AGE-2- and AGE-3-induced effects on the adhesion molecule expression, the cytokine production, and the lymphocyte proliferation, but EP_1 and EP_3 receptor agonists had no effect. Moreover, we confirmed that a mixed EP_2/EP_4 receptor agonist, 11-deoxy-PGE_1 (Suzawa et al., 2000; Noguchi et al.,

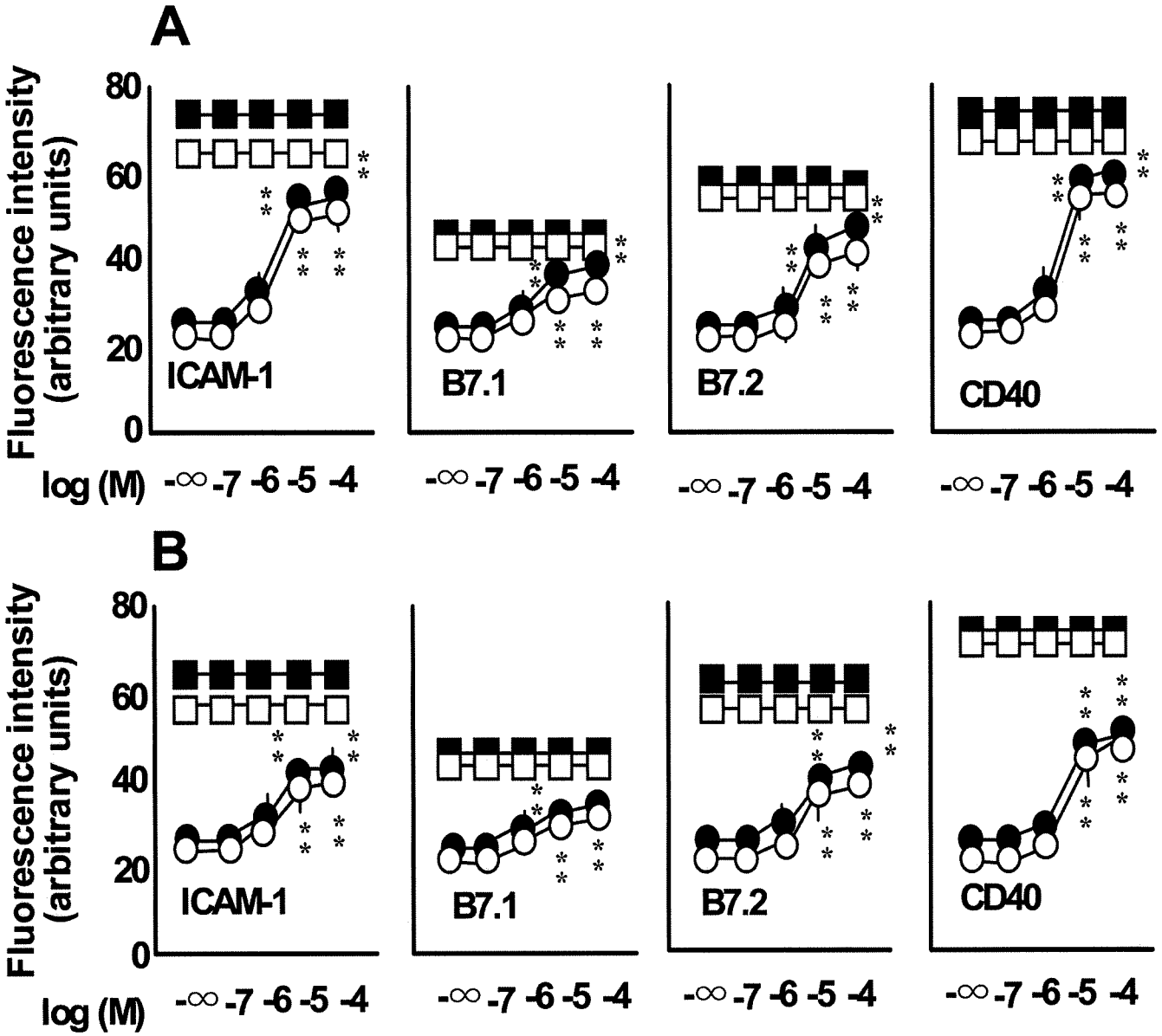

Fig. 6. The effects of prostanoid receptor antagonists on the inhibitory effect of PGE_2 on the expressions of ICAM-1, B7.1, B7.2, and CD40 PBMC at 1×10^6 cells/ml treated with PGE_2 at 1 μM were incubated with the EP_2 receptor antagonist, AH6809 (A), and the EP_4 receptor antagonist, AH23848 (B), at increasing concentrations from 0.1 to 100 μM in the presence of AGE-2 and AGE-3 at 100 μg/ml. The expressions of ICAM-1, B7.1, B7.2, and CD40 on monocytes were determined by flow cytometry. Filled circles (●) represent the effect of antagonists on PGE_2-inhibited adhesion molecule expression in the presence of AGE-2. Open circles (○) represent the effect of antagonists on PGE_2-inhibited adhesion molecule expression in the presence of AGE-3. Filled squares (■) represent the effect of antagonists on the actions of AGE-2 in the absence of PGE_2. Open squares (□) represent the effect of antagonists on the actions of AGE-3 in the absence of PGE_2. The results are expressed as the means ± S.E.M. of five donors with triplicate determinations. **, $P < 0.01$ compared with the values for PGE_2 in the presence of AGE-2 and AGE-3. When an error bar was within a symbol, the bar was omitted.

2001), inhibited AGE-2- and AGE-3-induced adhesion molecule expression in a concentration-dependent manner (Fig. 5). Moreover, the effect of an EP_2 receptor antagonist, AH6809 (Kay et al., 2006), and an EP_4 receptor antagonist, AH23848 (Kay et al., 2006), at concentrations ranging from 0.1 to 100 μM, on the adhesion molecule expression, cytokine production, and lymphocyte proliferation was examined in the presence of PGE_2 at 1 μM (Figs. 6 and 7). AH6809 and AH23848 reversed the inhibitory effect of PGE_2 on AGE-2- and AGE-3-induced expressions of ICAM-1, B7.1, B7.2, and CD40, the production of IFN-γ and TNF-α, and the lymphocyte proliferation in a concentration-dependent manner. On the other hand, AH6809 and AH23848 had no effect on the actions of AGE-2 and AGE-3 in the absence of PGE_2.

Effects of PGE_2 on the Production of cAMP in Monocytes in the Presence or Absence of AGE-2 and AGE-3. The effects of PGE_2 at 10 nM on the production of intracellular cAMP in monocytes isolated from PBMC in the presence (100 μg/ml) or absence of AGE-2 and AGE-3 were determined (Fig. 8). PGE_2 induced the production of cAMP in monocytes at a peak 30 min after stimulation. The presence of AGE-2 and AGE-3 did not influence the production of camp

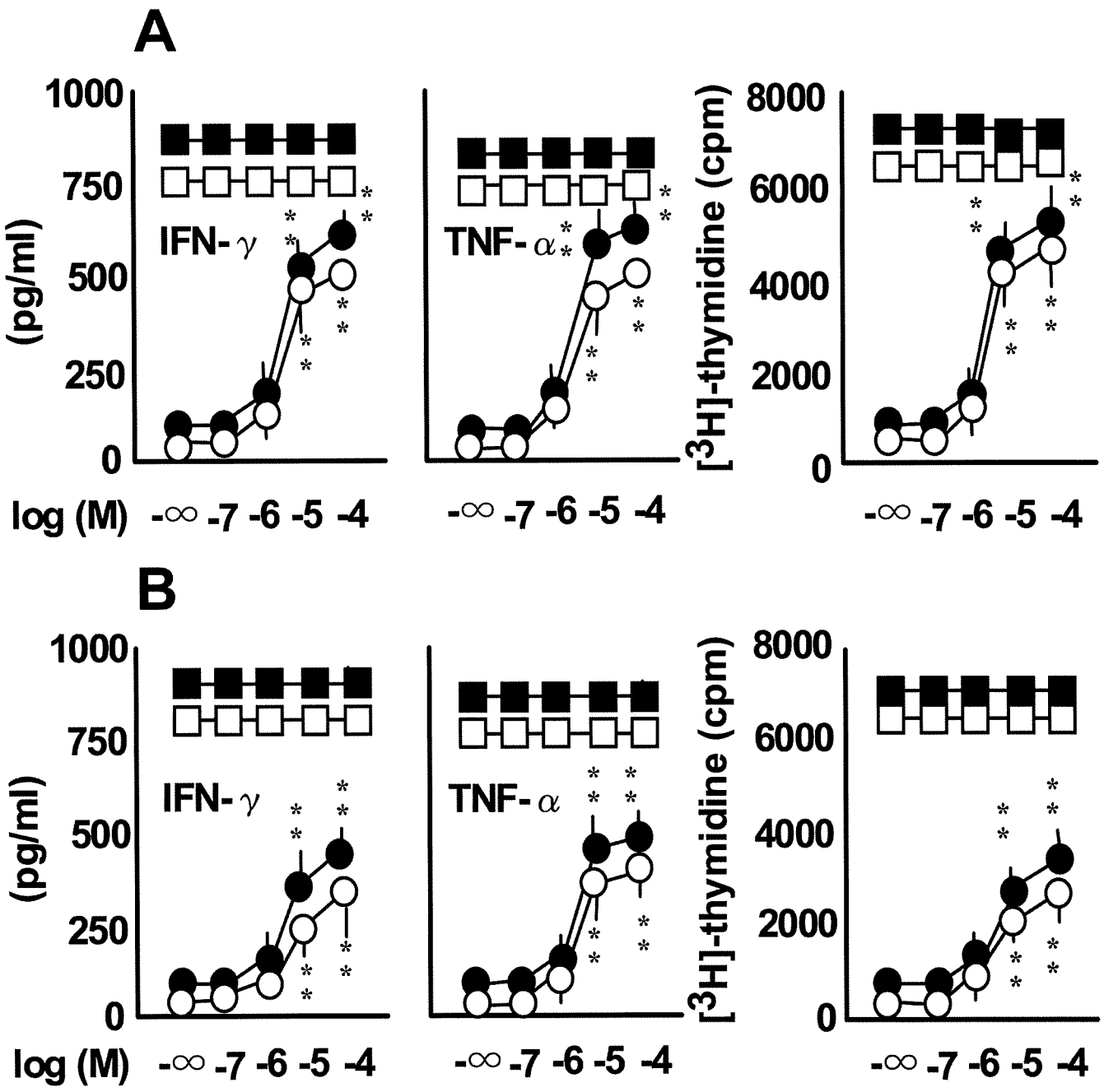

Fig. 7. The effects of prostanoid receptor antagonists on the inhibitory effect of PGE_2 on the production of IFN-γ and TNF-α and the lymphocyte proliferation PBMC at 1×10^6 cells/ml treated with PGE_2 at 1 μM were incubated with the EP_2 receptor antagonist, AH6809 (A), and the EP_4 receptor antagonist, AH23848 (B), at increasing concentrations from 0.1 to 100 μM in the presence of AGE-2 and AGE-3 at 100 μg/ml. IFN-γ and TNF-α concentrations in conditioned media were determined by ELISA. The lymphocyte proliferation was determined by [^{3}H]thymidine uptake as described under *Materials and Methods*. Filled circles (●) represent the effect of antagonists on PGE_2-inhibited adhesion molecule expression in the presence of AGE-2. Open circles (○) represent the effect of antagonists on PGE_2-inhibited adhesion molecule expression in the presence of AGE-3. Filled squares (■) represent the effect of antagonists on the actions of AGE-2 in the absence of PGE_2. Open squares (□) represent the effect of antagonists on the actions of AGE-3 in the absence of PGE_2. The results are expressed as the means ± S.E.M. of five donors with triplicate determinations. **, $P < 0.01$ compared with the values for PGE_2 in the presence of AGE-2 and AGE-3. When an error bar was within a symbol, the bar was omitted.

induced by PGE_2. EP_2 and EP_4 receptor agonists at 10 nM induced the production of camp (Fig. 8).

Involvement of cAMP in the Actions of PGE_2. To investigate the involvement of the cAMP/protein kinase A (PKA) pathway in the effects of PGE_2 on the expressions of ICAM-1, B7.1, B7.2, and CD40, the production of IFN-γ and TNF-α, and the lymphocyte proliferation, the effect of a PKA inhibitor, H89, at concentrations ranging from 0.1 to 100 μM, on the actions of PGE_2 in the presence of AGE-2 and AGE-3 at 100 μg/ml was determined (Figs. 9 and 10). H89 reversed the inhibitory effect of PGE_2 on AGE-2- and AGE-3-induced expressions of ICAM-1, B7.1, B7.2, and CD40, the production of IFN-γ and TNF-α, and the lymphocyte proliferation. On the other hand, H89 had no effect on the actions of AGE-2

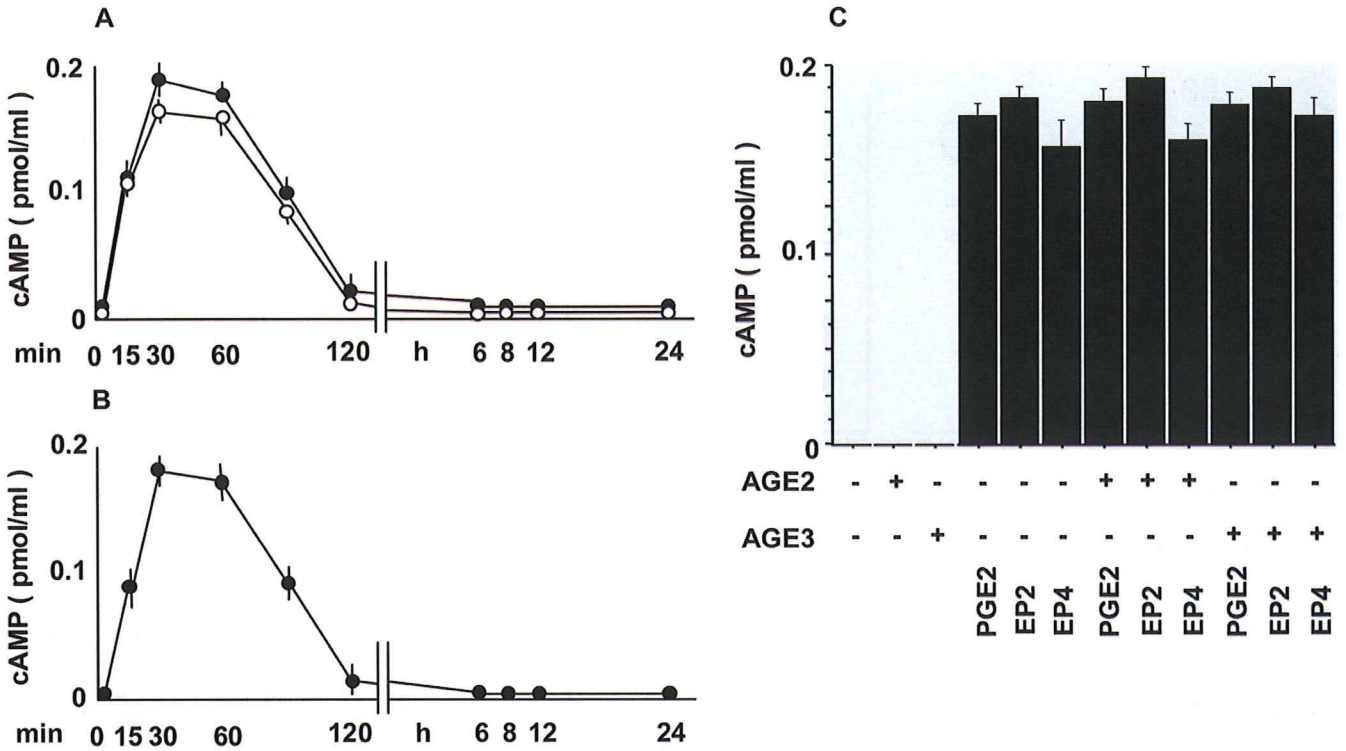

Fig. 8. The effects of PGE_2 on the production of cAMP in monocytes in the presence or absence of AGE-2 and AGE-3. A, monocytes at 1×10^6 cells/ml were incubated with PGE_2 at 10 nM in the presence (filled circles; ●) and absence (open circles; ○) of AGE-2 (A) and AGE-3 (B) at 100 μg/ml, and the time course changes in the levels of cAMP in monocytes were determined at the indicated time points. C, the effect of PGE_2, the EP_2 receptor agonist, ONO-AE1-259-01, and the EP^3 receptor agonist, ONO-AE-248, at 10 nM on the production of cAMP in the presence or absence of AGE-2 and AGE-3 at 30 min was determined. The results are expressed as the means ± S.E.M. of five donors with triplicate determinations. ND, not detected. When an error bar was within a symbol, the bar was omitted.

and AGE-3 in the absence of PGE_2. As shown in Figs. 11 and 12, the effects of a membrane-permeable cAMP analog, db-cAMP, and an adenylate cyclase activator, forskolin, at concentrations ranging from 0.1 to 100 μM, on the expressions of ICAM-1, B7.1, B7.2, and CD40 on monocytes, the production of IFN-γ and TNF-α, and the lymphocyte proliferation in PBMC in the presence of AGE-2 and AGE-3 at 100 μg/ml were examined. Both dbcAMP and forskolin inhibited AGE-2- and AGE-3-induced adhesion molecule expressions, the cytokine production, and the lymphocyte proliferation in a concentration-dependent manner.

Discussion

The level of glyceraldehyde-derived AGE (AGE-2) is reported to be 17 μg/ml in the serum of patient with diabetes (Enomoto et al., 2006; Nakamura et al., 2007). It is reported that AGEs at the concentrations ranging from 50 to 200 μg/ml remarkably induce human monocyte adhesion to bovine retinal endothelial cells (Mamputu et al., 2004). AGEs at 200 μg/ml induce the expression of CD40, CD80, and CD86 and the production of IFN-γ in dendritic cells (Ge et al., 2005). In the previous study, we found that AGE-2 and AGE-3 at 10 and 100 μg/ml significantly up-regulated the expressions of ICAM-1, B7.1, B7.2, and CD40, the production of IFN-γ and TNF-α, and the lymphocyte proliferation (Takahashi et al., 2009). Thus, the concentration used in the present study covers the pathological concentration of AGEs reported in the studies (Enomoto et al., 2006; Nakamura et al., 2007). Moreover, the accumulation of AGEs is shown in the atherosclerotic lesion by immunohistochemistry (Nakamura et al., 1993). It is probably that higher concentrations of AGEs may be present in the specific inflammatory lesions. Therefore, we determined the effects of AGEs at rather high pharmacological concentration (100 μg/ml).

In the present study, we found, for the first time, that PGE_2 inhibited AGE-2- and AGE-3-induced expressions of ICAM-1, B7.1, B7.2, and CD40, the production of IFN-γ and TNF-α, and the lymphocyte proliferation (Figs. 1 and 2). It is suggested that PGE_2 modulates inflammation during atherogenesis and other inflammatory diseases by suppressing macrophage-derived chemokine production via the EP_4 receptor (Takayama et al., 2002). To investigate receptor subtypes involved in the action of PGE_2, we used selective agonists for respective receptors (Suzawa et al., 2000). The EP_2 receptor agonist, ONO-AE1-259-01, and the EP_4 receptor agonist, ONO-AE1-329, were shown to be highly selective for mouse EP_2 and EP_4 receptors, respectively, using a receptor binding assay for Chinese hamster ovary cells transfected with each EP cDNA (Suzawa et al., 2000). It is reported that the selective EP_1, EP_2, EP_3, and EP_4 receptor agonists used in the present study were highly selective for their respective receptors (Suzawa et al., 2000). For example, the EP_2 receptor agonist, ONO-AE1-259, had at least 700-fold higher affinity for EP_2 receptors compared with other receptor agonists (Suzawa et al., 2000). As shown in Figs. 3 and 4, ONO-AE1-259 and ONO-AE-1-329 mimicked the effects of PGE_2 on the adhesion molecule expression, the cytokine pro-

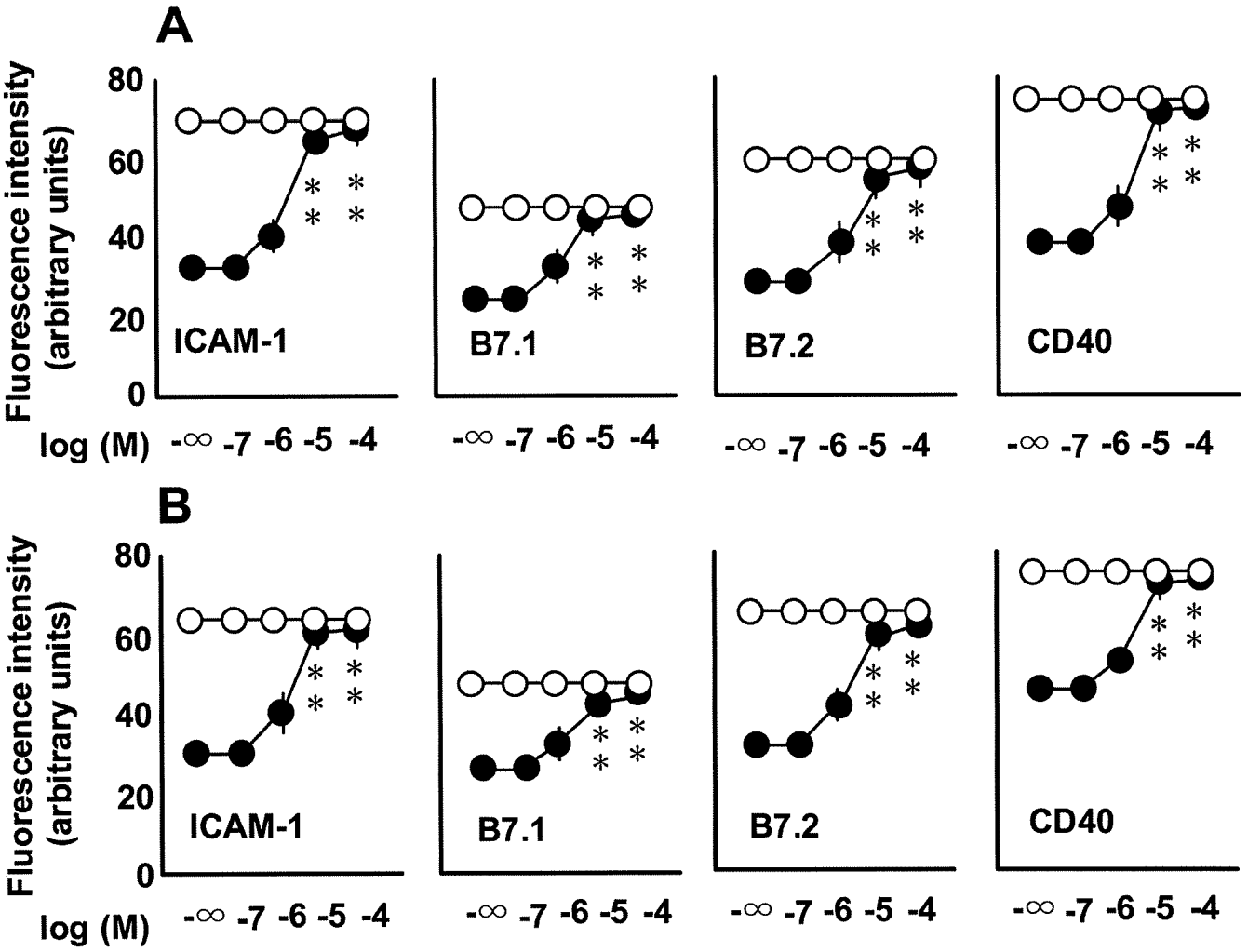

Fig. 9. The effects of PKA inhibitor on PGE_2-inhibited ICAM-1, B7.1, B7.2, and CD40 expressions. The effect of a PKA inhibitor, H89, at increasing concentrations from 0.1 to 100 μM on the expressions of ICAM-1, B7.1, B7.2, and CD40 on monocytes treated with PGE_2 at 10 nM in the presence of the AGE-2 (A) and AGE-3 (B) at 100 μg/ml was determined by flow cytometry. Filled circles (●) represent the effects of H89 on the PGE_2-induced inhibition of responses in the presence of AGE-2 and AGE-3. Open circles (○) represent the effects of H89 in the presence of AGE-2 and AGE-3 without PGE_2 stimulation. The results are expressed as the means ± S.E.M. of triplicate findings from five donors. **, $P < 0.01$ compared with the value for PGE_2. When an error bar was within a symbol, the bar was omitted.

duction, and the lymphocyte proliferation. In the present study, IC_{50} values for the inhibitory effects of ONO-AE1-259 and ONO-AE-1-329 on the expression of ICAM-1 on monocytes induced by AGE-2 and AGE-3 were similar, respectively (Table 1). It is unlikely that either receptor agonist stimulated the other receptors at the concentration range used judging from the selectivity of each agonist. As shown in Fig. 5, the observation that the mixed EP_2/EP_4 receptor agonist, 11-deoxy-PGE_1 (Noguchi et al., 2001), mimicked the inhibition of AGE-2- and AGE-3-induced adhesion molecule expression by PGE_2 was consistent with the above conclusion. Because the IC_{50} values of PGE_2 to prevent the upregulation of adhesion molecule expressions, cytokine production, and lymphocyte proliferation were consistent with the affinity of those agonists to typical EP_2 and EP_4 receptors (Table 1) (Takahashi et al., 2002). Moreover, the EP_2 receptor antagonist, AH6809, and the EP_4 receptor antagonist, AH23848, inhibited the actions of PGE_2 (Figs. 6 and 7). Therefore, it was suggested that the inhibitory effect of PGE_2 was mediated by the stimulation of EP_2 and EP_4 receptors but not EP_1 and EP_3 receptors.

It is known that the stimulation of EP_2 and EP_4 receptors induces the production of cAMP (Coleman et al., 1994). As shown in Fig. 8, PGE_2, EP_2, and EP_4 receptor agonists induced the production of cAMP in monocytes irrespective of the presence of AGE-2 and AGE-3. The PKA inhibitor, H89, inhibited the action of PGE_2 (Figs. 9 and 10), and the cAMP analog, dbcAMP, and the adenylate cyclase activator, forskolin, mimicked the effect of PGE_2 (Figs. 11 and 12). These results suggested the involvement of the EP_2/EP_4 receptor-cAMP/PKA pathway in the actions of PGE_2. In addition, the present data were consistent with the finding that the elevation of cAMP prevents the production of TNF-α in monocytes of diabetic patients (Jain et al., 2002). We observed a similar pattern of the inhibitory effects of PGE_2 on IL-18-induced activation of monocytes in human PBMC via EP_2 and EP_4 receptors (Takahashi et al., 2002). Thus, there may be a common pathway triggered by IL-18 and AGEs that was

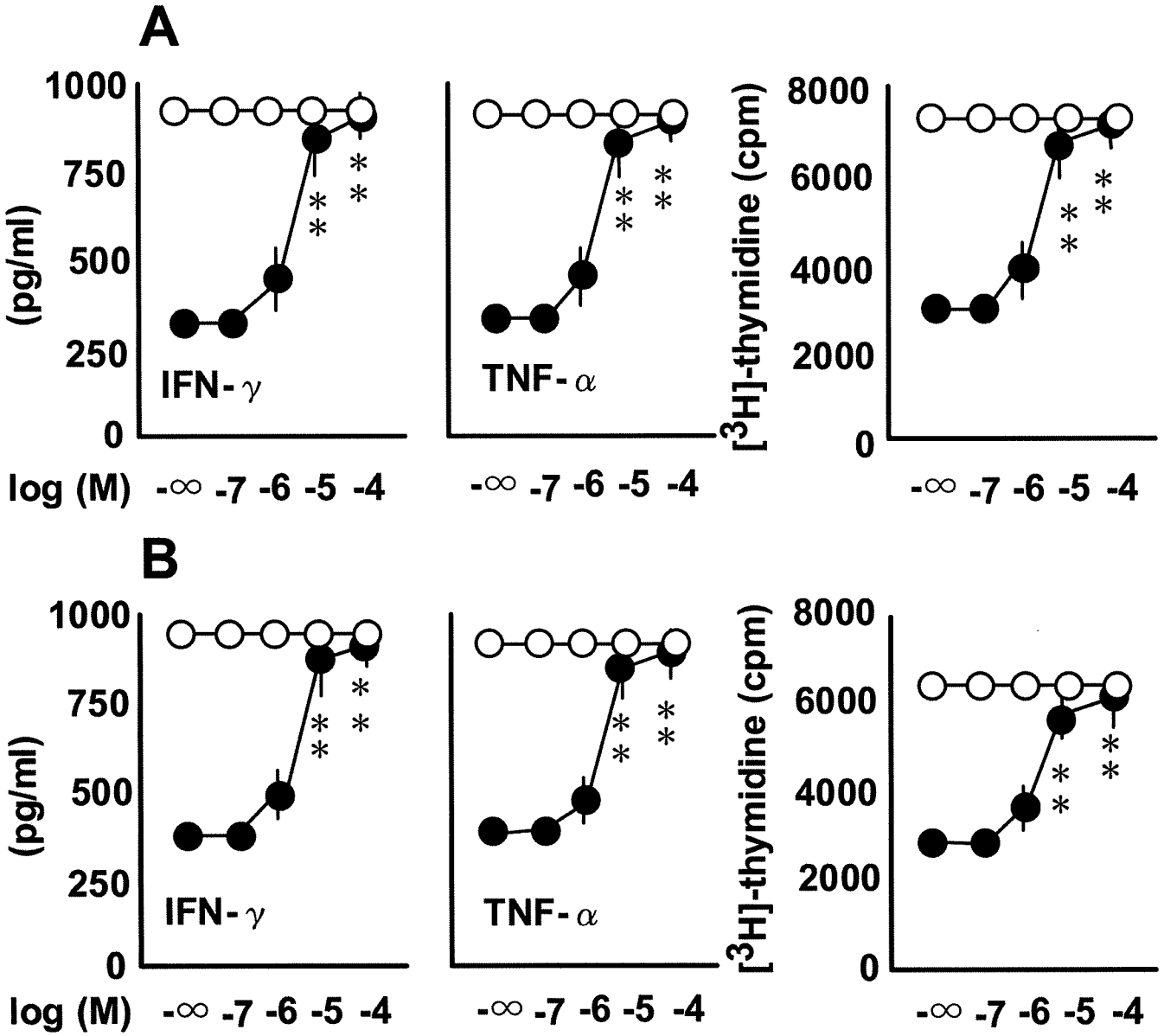

Fig. 10. The effects of PKA inhibitor on PGE_2-inhibited TNF-α and IFN-γ production and the lymphocyte proliferation. The effect of a PKA inhibitor, H89, at increasing concentrations from 0.1 to 100 μM on the production of TNF-α and IFN-γ in PBMC treated with PGE_2 at 10 nM in the presence of AGE-2 (A) and AGE-3 (B) at 100 μg/ml was determined by ELISA. The lymphocyte proliferation was determined by [^{3}H]thymidine uptake as described under *Materials and Methods*. Filled circles (●) represent the effects of H89 on the PGE_2-induced inhibition of responses in the presence of AGE-2 and AGE-3. Open circles (○) represent the effects of H89 in the presence of AGE-2 and AGE-3 without PGE_2 stimulation. The results are expressed as the means ± S.E.M. of triplicate findings from five donors. **, $P < 0.01$ compared with the value for PGE_2. When an error bar was within a symbol, the bar was omitted.

regulated by the EP_2/EP_4 receptor-cAMP/PKA system. Further work is necessary on this issue.

In the previous study, we found that AGE-2 and AGE-3 had higher affinity for RAGE than AGE-4 and AGE-5 using an in vitro binding assay (Takahashi et al., 2009). AGE-2 and AGE-3, but not AGE-4 and AGE-5, induced the up-regulation of their receptor RAGE expression on the cell surface of monocytes. PGE_2 had no effect on the expression of RAGE in the presence and absence of AGE-2 and AGE-3 (data not shown), suggesting that there might be distinct signal transduction pathways of RAGE activation, leading to enhanced expression of adhesion molecule and RAGE, which were differentially regulated by the cAMP/PKA system.

RAGE is predominantly localized with lesional macrophages in human carotid atherosclerotic plaques, where macrophages also represent the majority of COX-2-expressing cells (Cuccurullo et al., 2006). It is reported that AGEs ligate cell-surface RAGE on the vascular endothelium, mononuclear phagocytes, vascular smooth muscle, and neurons to activate cell signaling pathways such as P44/P42 mitogen-activated protein kinase and NF-κB (Yan et al., 1994; Lander et al., 1997), redirecting cellular function in a manner linked to the expression of inflammatory and prothrombotic genes important in the pathogenesis of chronic disorders such as diabetic microvascular disease and amyloidosis (Schmidt et al., 1994; Miyata et al., 1996; Park et al., 1998). When stim-